Patrícia Sofia Sousa Dias

Polyglutamine diseases (PolyQ): construction and characterization of yeast models

LISBOA

2011

nº de arquivo
“Copyright”

UNIVERSIDADE NOVA DE LISBOA

FACULDADE DE CIÊNCIAS E TECNOLOGIA

DEPARTAMENTO DE CIÊNCIAS DA VIDA

Patrícia Sofia Sousa Dias

Polyglutamine diseases (PolyQ): construction and characterization of yeast models

Dissertação apresentada para a obtenção do Grau de Mestre em Genética Molecular e Biomedicina, pela Universidade Nova de Lisboa, Faculdade de Ciências e Tecnologia

Orientador:
Profª. Doutora Paula Ludovico (ECS/UM)

LISBOA
2011

Agradecimentos

No fim desta longa caminhada, não poderia acabar sem agradecer às pessoas que de diferentes maneiras possibilitaram que hoje estivesse a escrever a última página da minha tese.

Gostaria de agradecer à Professora Cecília Leão que deu o meu contacto à Professora Drª Paula Ludovico. À Professora Drª Paula Ludovico, que me aceitou no seu grupo e que me deu todas as orientações para conseguir desenvolver o meu trabalho e acabar a minha tese. Não menos importante é o agradecimento que quero fazer à pessoa que esteve comigo no laboratório com quem discuti ideias e resultados. Este agradecimento vai para a Belém.

Um muito obrigado aos meus colegas de grupo Alexandra, Ana e Henrique como também a todos aqueles que estiveram dia-a-dia comigo no laboratório, "Gina", João Menino, Sandra, Júlia e Tiago. A todos eles agradeço todo o apoio que me deram, todos os momentos bons passados no laboratório e fora dele, todo o apoio dado nos meus momentos maus ouvindo-me e aturando-me a falar das coisas menos boas que ocorreram, e principalmente a ajuda que me deram e o que me ensinaram durante esta longa caminhada.

Quero também agradecer às minhas colegas de casa, que se tornaram boas amigas, que me ouviram mesmo sem perceber o que dizia sobre as minhas experiências boas ou menos boas, que me apoiaram e que acima de tudo me animaram nos dias mais complicados. Obrigada, Cristina, Elisabete, Fernanda e Cidália!

Um muito obrigada a todos os meus amigos, aqui de Braga, que trabalharam comigo no laboratório, e aos de Lisboa que sempre me aturaram e apoiaram. Principalmente a todos os meus amigos que deixei em Lisboa, um grande desculpa por não ter estado presente nos bons e maus momentos e por de certa forma ter-me afastado. Desculpem!

Dedico esta tese a toda a minha família, Pais, Mano, Avós, Madrinha e Tios. Estas foram as pessoas que me apoiaram psicologicamente durante todo este tempo. Mãe, Agradeço-te muito, muito mesmo por todos os momentos em que me ouviste por telefone, em que tentas-te dar-me apoio e por teres estado todos os dias ao meu lado, por telefone. Pai, um muito obrigada por também estares ao meu lado por me teres apoiado e ouvido, sinto que esta longa caminha nos uniu ainda mais. Avós, agradeço todo o vosso empenho em ouvir e apoiarem-me, e peço muita desculpa por quase não estar com vocês e pelos momentos em que estive mas que foram sempre a correr. Madrinha, apesar de estares longe de nós, agradeço todas as vezes em que falamos e nas quais sempre me apoiaste e

me deste ânimo para continuar. Tios, um muito obrigada por sentir o vosso apoio. Quero também fazer um agradecimento especial ao meu irmão. Tiago apesar de seres pequenino, sempre que estava contigo esquecia-me das coisas e sempre que brincava contigo ficava mais contente.

Um **Muito Obrigada** a todos!!!!!!!

Table of Contents

Table of Contents

Abbreviations

ATG	Autophagy related genes
BDNF	Brain-derived neurotrophic factor
cDNA	Complementary DNA
CFUs	Colony-forming units
CLS	Chronological life span
CTV	Cytoplasm-to-vacuole pathway
dNTP	Deoxyribonucleotide
DNA	Deoxyribonucleic acid
DUB	Deubiquitination enzyme
EDTA	Ethylenediaminetetraacetic acid
ER	Endoplasmic reticulum
ERAD	Endoplasmic Reticulum Associated Protein Degradation
GABA	γ-Aminobutyric acid
GFP	Green fluorescent protein
HD	Huntington's disease
HEAT	Huntingtin, elongation factor 3 (EF3), protein phosphatase 2A (PP2A), and the yeast PI3-kinase TOR1
Hsp	Heat shock protein
IgG	Immunoglobulin G
JD	Josephin domain
JNK	c-Jun N-terminal kinase
KCl	potassium chloride
LB	Lysogeny broth
MAP	Mitogen-activated protein kinase
$MgCl_2$	Magnesium chloride
MJD	Machado-Joseph's disease
NaCl	Sodium chloride
NaOH	Sodium hydroxide
NES	Nuclear export sequence

Abbreviations

NLS	Nuclear localization sequence
PCR	Polymerase chain reaction
PMSF	Phenylmethanesulfonyl fluoride
polyQ	Polyglutamine
QC	Quality control
RNA	Ribonucleic acid
REST/NRSF	RE1-Silencing Transcription factor/Neuron-Restrictive Silencer Factor
RLS	Replicative life span
ROS	Reactive oxygen species
SDS	Sodium dodecyl sulfate
SOC	Super Optimal broth with Catabolite repression
SUMO	Small Ubiquitin-like Modifier
TFIID	Transcription factor II D
TFIIF	Transcription factor II F
TAE	Tris-acetate-EDTA
TBS	Tris Buffered Saline
Tris	2-Amino-2-hydroxymethyl-propane-1,3-diol
YEPD	Yeast Extract Peptone Dextrose

Abstract

There are a number of serious diseases which have in common the inappropriate folding of a particular protein, as polyglutamine disease group. Machado-Joseph's and Huntington's disease are grouped in the polyglutamine diseases, being the cause of the disease the presence of a CAG repeat tract in the causative gene, ATXN3 and HTT, respectively. This CAG repeats tract leads to the formation of polyglutamine tract in ataxin-3 and huntingtin proteins, respectively, that do not allow the correct protein folding. In diverse models, the expansion of the poluglutamine tract into disease related-proteins, promote their aggregation and their negative effect on cellular metabolism were described as associated to toxic effect.

In this study, it was proposed the construction of the first yeast model for Machado-Joseph's disease and the characterization of the role of autophagy in the yeast model for Huntington's disease during yeast life cycle. For the yeast model for Machado-Joseph's disease we successfully constructed a Tet On system harboring the variant 1 genes, normal and expanded, fused with GFP gene, to further allow the subcellular localization of the expressed protein into yeast cells. In yeast model for Huntington's disease the chronological lifespan (CLS) of yeast cells at different physiological states after expressing the normal and the pathogenic protein and their subcellular localization, using epifluorescent microscopy was studied. It was demonstrated that cells harboring the huntingtin with 103 glutamines (pathogenic protein) during the inhibition of autophagic process, by chloroquine, presents an increased in CLS and the formation of large foci that could correspond to aggregosomes. In aged cells this effect is more pronounced leading to the hypothesis that in these cells the autophagic mechanism is impaired and enhances the toxic effects of expressed huntingtin 103Q and that the inhibition of the autophagic process can rescue the cells from the toxic effects. On the other hand, when the normal huntingtin (25Q) was expressed at exponential phase the inhibition of autophagy led to a drastic decrease on CLS, demonstrated that in functional cells the autophagy had a positive effect being a crucial process, probably removing unwanted intracellular components and providing energy.

Resumo

Há um número de doenças graves que têm em comum a conformação inapropriada de certas proteínas, como o grupo das doenças poliglutâmicas. As doenças de Machado-Joseph e de Huntington fazem parte deste grupo de doenças, sendo a sua causa a presença de um tracto de repetições CAG no gene responsável pela doença, ATXN3 e HTT genes, respectivamente. Este tracto de repetições CAG leva à formação de um tracto de poluglutaminas nas proteínas ataxina-3 e huntingtina, respectivamente, não permitindo a sua conformação correcta. Em diversos modelos foi já descrita a toxicidade causada pela expansão do tracto de poliglutaminas tal como a sua agregação e o efeito negativo no metabolismo celular.

Neste estudo, foi proposta a construção do primeiro modelo de levedura para a doença de Machado-Joseph tal como a caracterização do modelo de levedura para a doença de Huntington, ao longo do ciclo de vida das leveduras, com inibição da autofagia pelo antibiótico cloroquina. Para o modelo de levedura para a doença de Machado-Joseph foi construído com sucesso um sistema Tet On com os genes normal e expandido da variante 1 em fusão com o gene GFP, que permitirá analisar a localização celular das proteínas após expressão em células de levedura. No modelo de levedura para a doença de Huntington foi analisada a longevidade cronológica das células em diferentes estados fisiológicos após expressão da proteína normal e patogénica como também a sua localização celular, através de microscopia de epifluorescência. Demonstrou-se que as células que expressavam a proteína huntingtina com 103 glutaminas (proteína patogénica) durante a inibição do processo autofágico, pela cloroquina, apresentam um aumento da longevidade cronológica e a formação de grandes *foci* que podem corresponder aos agregosomas. Nas células envelhecidas o efeito do aumento da longevidade cronológica, após inibição da autofagia, é mais pronunciado levantando-se a hipótese de que nestas células o mecanismo autofágico estará alterado aumentando o efeito tóxico da expressão da huntingtina patogénica e que a inibição da autofagia pode recuperar as células do efeito tóxico. Por outro lado, quando a huntingtina normal (com 25 glutaminas) é expressa em fase exponencial a inibição da autofagia leva a uma diminuição drástica da longevidade cronológica, demonstrando que em células funcionais a autofagia tem efeito positivo sendo um processo crucial, provavelmente removendo componentes celulares indesejáveis e fornecendo energia.

I. Introduction

I. Introduction

1. Protein misfolding diseases

Proteins are by far the most structurally complex and functionally sophisticated biomolecules known. Proteins have a unique three-dimensional structure or conformation that is achieved by their correct folding. The protein folding initiates when nascent chain is still attached to ribosome. These nascent chains, or the newly synthesized proteins, might fold correctly into their three-dimensional structure on their own and maintain these native states throughout their lifetime. However, mutations or errors in transcription, RNA splicing and translation may lead to slowly folding protein or to a protein that will never achieve the correct folding. Incompletely or abnormal folded proteins expose their hydrophobic patches. Thus, cells have evolved mechanisms that recognize and remove the hydrophobic patches helping proteins to refold. Molecular chaperones, such as heat-shock proteins (HSP) recognized the exposed hydrophobic patches acting as a first defense to help on protein folding. The incompletely folded proteins, accumulates in endoplasmic reticulum (ER) when attempts to refold a protein fails, it is also marked for destruction by ER-association protein degradation (ERAD), a process that involves the protein retrotranslocation into cytosol and proteasome-mediated proteolysis (Barral *et al.,* 2004). The molecular chaperones and the proteasome-mediated proteolysis processes function concurrently to prevent massive protein misfolding accumulation (Figure 1) (Alberts *et al.*, 2002).

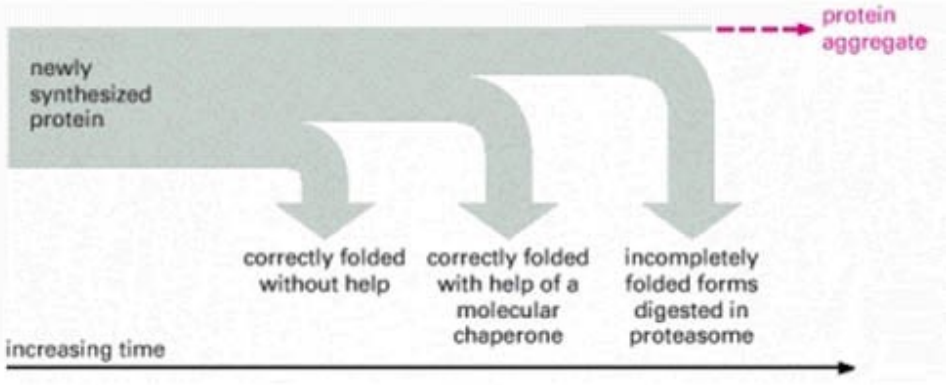

Figure 1. The cellular mechanisms of protein quality control after protein synthesis (from Alberts *et al.*, 2002).

The misfolded proteins may be nonfunctional or suboptimally funtional, or they may be degraded by cellular machinery or the misfolding ones may expose epitopes which lead to dysfunctional interactions with other proteins causing protein aggregation in the aqueous cellular environment. Accumulation of aggregates can disrupt cellular trafficking and degradation process leads to the formation of toxic protein precipitates, inactivation of functional proteins and ultimately cell death (Gao and Hu, 2008).

Protein misfolding leads to the malfunctioning of the living systems. There are a number of serious diseases which have a common aspect that appear to involve inappropriate folding of a particular protein. Neurodegenerative diseases (Table I) are directly or indirectly caused by aberrant protein folding and aggregation (Lee and Yu, 2005). The hallmark of these disorders is the presence of cytosolic, nuclear and extracellular protein aggregates, which are toxic for the cell leading to the alterations of cellular activities and promoting the activation of cell death signaling pathways. Furthermore, it is also thought that these disorders are the result of the acquisition of dominant toxic functions by aberrantly folded proteins (Barral *et al.*, 2004) as a gain of function of the protein related disease. The accumulation of toxic misfolded proteins, in these disorders, may overload the cellular chaperone capacity, thus giving rise to disease phenotypes. Moreover, these disease phenotypes increase in severity with age, when changes in the intracellular environment reduce the efficiency of the quality control machinery (Barral *et al.,* 2004).

Table I. Examples of human conformational diseases caused by protein deposits (Lee and Yu, 2005).

Disease	Disease proteins	Characteristic pathology
Familial encephalopathy with neuroserpin inclusion bodies	Neuroserpin	Collins body formation; neuronal inclusions
α_1-antitrypsin deficiency	α_1-antitrypsin	Inclusions in hepatocytes leading to emphysema, liver cirrhosis
Alzheimer's disease	Amyloid β-protein and hyperphosphorylated tau	Extracellular plaques; Tangles in neuronal cytoplasm
Parkinson's disease	α-synuclein	Lowy body formation
Creutzfeldt-Jakob disease	Prion protein (PrP^{sc})	Spongiform degeneration; extracellular plaques; amyloid inside and outside neurons
Huntington's disease and other polyglutamine expansion disease	Long glutamine stretches within certain proteins	Intranuclear inclusions and cytoplasmic aggregates

Among the different neurodegenerative diseases caused by aberrant protein folding, the polyglutamine-expanded disorders, Huntington's and Machado-Joseph diseases will be focused in the next section.

2. Machado-Joseph's disease

Machado-Joseph's disease was first reported in North American families of Portuguese-Azorean ancestry. This is a slowly progressive neurodegenerative disease and the patients present a wide range of clinical manifestations that include cerebellar ataxia, pyramidal signs, dystonia, progressive external ophtalmoplegia and peripheral neuropathy and will became confined to a wheelchair and later bedridden (Kawai *et al.,* 2004). The neuropathology consists in the neuronal loss of gray matter on multiple areas, such as the pontine noroadrenegic system and the dopaminergic and cholinergic midbrain, in white matter degeneration was restricted to the cerebellum, spinal cord and brainstem (reviewed in D'Abreu *et al.,* 2010). It is a hereditary autossomal dominant disease, meaning that the inheritance of one copy of the ATXN3 gene, from an affect parent, will lead to the development of the disease. Takiyama and colleagues, using highly polymorphic microsatellite DNA polymorphism, assigned the MJD1 (ATXN3) gene to the long arm of chromosome 14 (14q24.3-q32.1) by genetic linkage to microsatellite loci D14S55 and D14S48 (Takiyama *et al.,* 1993).

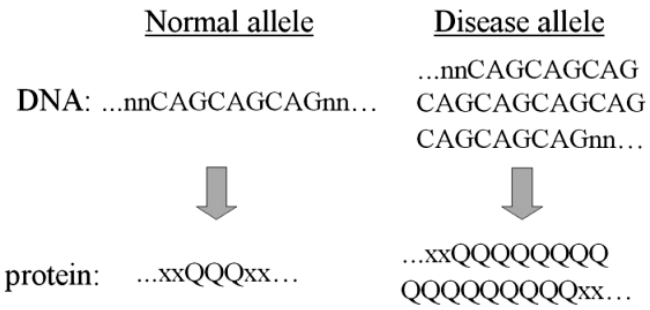

Figure 2. CAG tract in both normal and disease allele. The CAG repeats encodes for a glutamine tract in ataxin-3 protein, show here as Q, which is the single-letter amino acid code for glutamine (from Paulson, 2007).

A CAG repeat expansion found in the ATXN3 gene that encodes an expanded polyQ tract in the disease protein (Figure 2), known as ataxin-3 or MJDp, includes MJD into a class of related genetic disorders, the so-called expanded polyglutamine (polyQ) diseases (Kawaguchi *et al*, 1994).

The ATXN3 gene, responsible for MJD, is approximately 48,2 kb in size and is composed of 11 exons (Figure 3). The CAG repeats are found in exon 10, as represented in figure 3 (Ichikawa *et al*., 2001).

There are five described variants of ATXN3 gene (Ichikawa *et al.,* 2001). The first one, MJD1a, use exon 10 to provid the 3'-terminal sequence (Kawagushi *et al.*, 1994). The second group was previously described by Goto (Goto *et al.,* 1997), MJD2-1, is similar to MJD1a and carries a single nucleotide substitution in the stop codon.

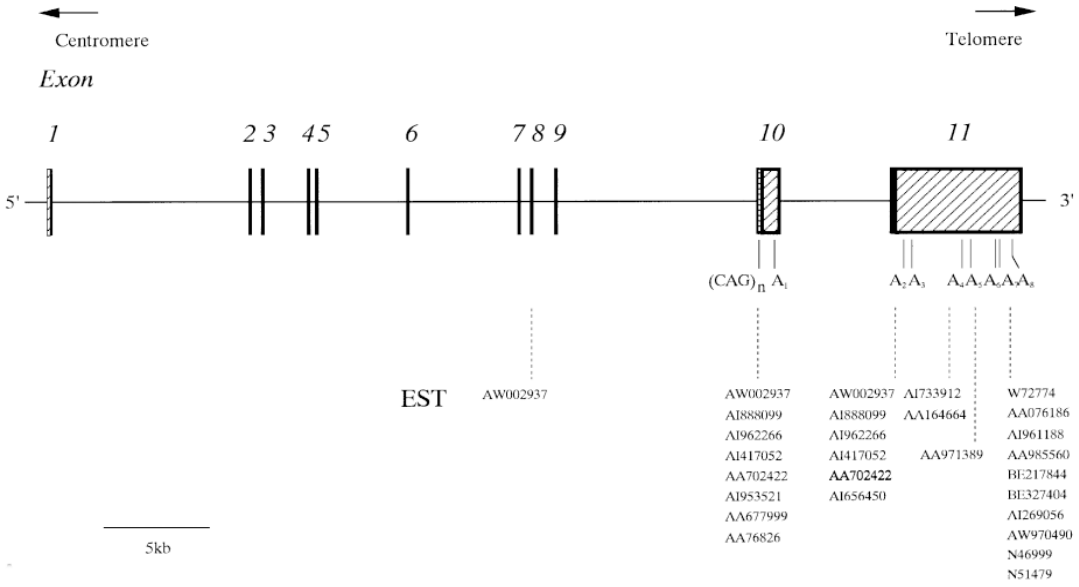

Figure 3. Genomic structure of ATXN3/MJD gene. Exons are numbered 1 to 11 and are represented as *boxes. Filled boxes* represent the coding region and hatched boxes represent the 5'- and 3'-untranslated regions (UTRs). *A1* to *A8* are polyadenylated consensus sequences (from Ichikawa *et al.,* 2001), shift in the open reading frame. And the last group is represented by a collection of clones that cannot be included in other groups, which formed the chimera cDNAs (from Ichikawa *et al.,* 2001).

The third group was described by Goto (Goto *et al.,* 1997), includes the MJD1-1 and MJD5-1, which skip 3' regions of exon 10 and employed exon 11 as 3'terminal sequence. In this group two distinct poliadenylation sites are created in the gene. There is a four group were exon 2 is absent, presumably by alternative splicing, but that do not cause a shift in the reading frame. The last group is represented by a collection of clones that cannot be included in other groups, which from the chimera cDNA (Ichikawa *et al.,* 2001). Ichikawa and colleagues observed that ATXN3 gene is ubiquitously transcribed in all adult human tissues, as human organs, brain and non-nervous tissues (Ichikawa *et al.,* 2001). More recently, Conceição Bettencourt and colleagues proposed that ATXN3 gene presents at least 56 possible alternative splicing variants generated by four types of splicing events (Bettencourt *et al.,* 2009). Despite the different isoforms, the ATXN3 gene encodes for a 42kDa protein, the ataxin-3. This protein presents a conserved globular deubiquitinating N-terminal Josephin domain (JD), followed by two or three Ubiquitin Interacting Motifs (UIMs), depending of the protein isoform and in C-terminal presents the CAG repeat tract (Figure 4) and the longest slice isoform of ataxin-3 has 376 amino acids (Albrecht *et al*., 2004).

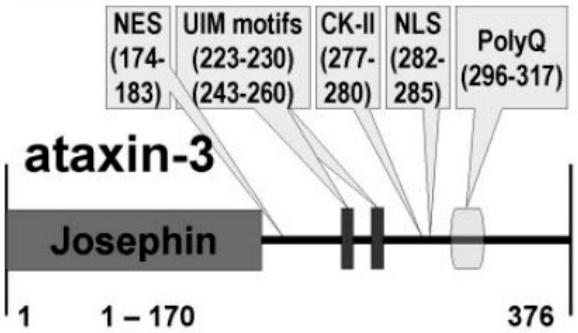

Figure 4. Protein architecture of human ataxin-3 (from Albrecht *et al*., 2004).

The individuals who are not affected present alleles containing from 12 to 37 repeats, whereas the affected individuals have at least one expanded allele, with sizes varying between 66 and 84 (Figure 5) (Maciel *et al*., 1995).

These affected individuals have an inverse correlation between age of disease onset and the CAG repeat length, meaning that these individuals have a tendency for age at onset to decrease as the CAG repeat length increases (Figure 5). During transmission from parent to offspring the CAG repeat length presents some instability (Figure 6) (Maciel *et al*., 1995). The poly-glutamine expansions (polyQ) are thought to cause a conformational chance in the polypeptide sequence promoting misfolding and aggregation of the disease protein. In MJD, it was described that ataxin-3 forms ubiquitinated intracellular aggregates or nuclear inclusions in selected populations of disease neurons (Paulson *et al.,* 1997). Although the pathogenic role of aggregations is controversial, protein misfolding, of disease protein, is generally thought to be crucial to pathogenesis raising the possibility that the cellular machinery that normally recognizes and handles misfolded proteins may play a role MJD.

Several studies were performed to dissect the machinery involving ataxin-3 protein on MJD.

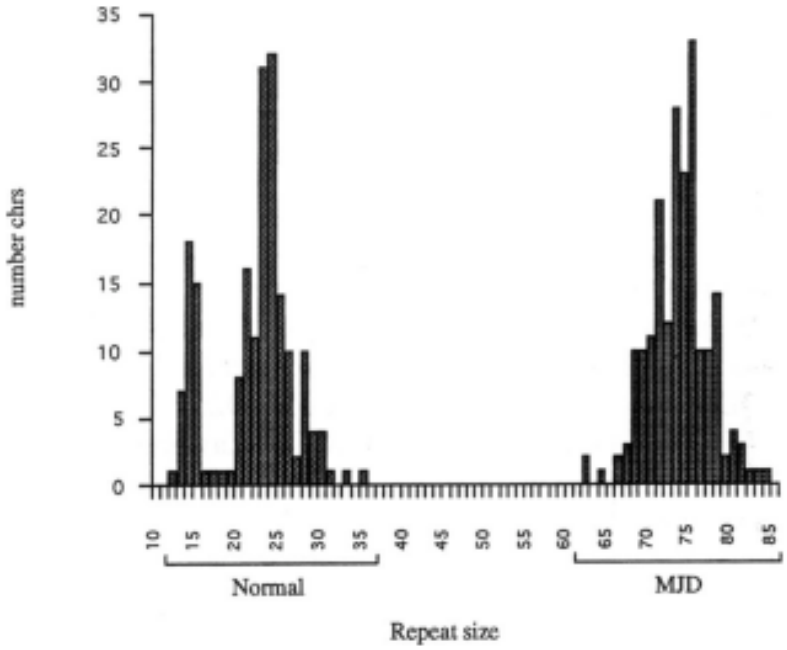

Figure 5. Distribution of CAG repeat sizes in unaffected control individuals and in MJD affected individuals (from Maciel *et al*., 1995).

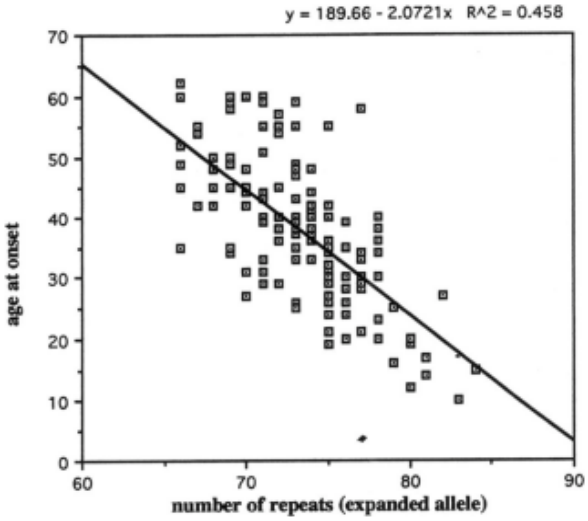

Figure 6. Correlation between CAG repeat lengths in the MJD chromosomes and age of onset. To this analysis were used 156 affected individuals with age at onset of disease (from Maciel *et al.,* 1995).

Burnett and colleagues, using an ubiquitin protease assay with ^{125}I-Lysozyme, demonstrated that ataxin-3 has ubiquitin protease activity, removing ubiquitin from growing chains and that cystein-14, from Josephin domain, is required for its activity (Burnett *et al.,* 2003). Using similar *in vivo* studies, Berke and colleagues not only confirmed that ataxin-3 has a ubiquitin protease activity and that binds polyubiquitin chains but also that normal and expanded ataxin-3 are degraded by the proteasome, defining that ataxin-3 has a function in the ubiquitin proteasome pathway (UPP) and that it is also regulated by this process (Berke *et al.,* 2005). In fact, it was described that ubiquitinated proteins and the proteasome complex redistributes into polyglutamine aggregates formed by the ataxin-3 (Chai *et al.,* 1999). These studies raise the possibility that expansion on CAG tract modulates ataxin-3 protease activity and/or the range of its substrates, being possible that expanded ataxin-3 acquires new properties that alter the UPP. Several proteins can bind ataxin-3, therefore is possible that ataxin-3 may act at the interface of these interactions and the UPP (Berke *et al.,* 2005).

Furthermore, some studies have shown that ataxin-3 interact with Rad23, that is a yeast homolog of human HHR23A and with Valosin-Containing Protein (VCP), that is a mammalian homolog of yeast cell cycle division protein Cdc48p (Doss-Pepe *et al.,* 2003 and Zhong and Pittman, 2006). These two proteins, Rad23 and VCP are involved on UPP. Rad23 play a role as a "shuttle factor" that translocate proteins to proteasome for degradation binding polyubiquitin chains through its ubiquitin-associated (UBA) domain. VCP is a member of AAA family of ATPases associated proteins with diverse cellular activities, including control of cell cycle division, vesicle-mediated transport and the UPP. In UPP, it is involved on ubiquitin-mediated proteolysis and has a role on endoplasmatic reticulum (ER)-associated degradation (ERAD) promoting the retranslocation of substrates from ER to the cytosol to be degraded (Zhong and Pittman, 2006). It was suggested that ataxin-3 compete with Ufd1 (protein from heterodímero responsible for extraction of proteins from ER) for binding to VCP impairing the binding of ubiquitilated ERAD substrates and decreasing their extraction from ER, promoting new cycles of folding and sorting the substrates into other quality control (QC) pathway. Biochemical data showed that mutated ataxin-3 binds VCP more efficiently than wild-type ataxin3, promoting a greater effect on ERAD inhibition, which may contribute to disease pathogenesis (Zhong and Pittman, 2006). The ataxin-3 properties link their normal function to protein surveillance pathways and suggest that alteration in normal ataxin-3, caused by the CAG expansion, could compromise protein homeostasis in the cell.

Pathological ataxin-3 is also involved on transcription process. Using transgenic mice expressing polyglutamine-expanded ataxin-3-Q79, Chou and colleagues, performed a microarray analysis and real-time PCR assays, from cerebellum, to test the involvement of expanded ataxin-3 on transcription. The microarrays indicated that genes involved in glutamatergic transmission, transcription factors, intracellular Ca^{++} signaling, heat shock proteins, GABA receptors and MAP kinase pathways are downregulated. While genes involved in pro-apoptotic response, cyclin and cyclin-dependent kinase 5, G protein subunits, proteasome subunits and RNA polymerase subunits are upregulated (Chou *et al*., 2008). It was previous described that ataxin-3 has a role in transcriptional repression, binding to CBP, p300 and PCAF coactivators, regulating transcription. N-terminal of ataxin-3 may also bind to histones and inhibit their acetylation by the transcription of

coactivators/HATs, acting on a new mechanism of transcriptional repression (Li *et al.,* 2002). Moreover, it is known that in early stages of disease the expanded ataxin-3 is associated with the mitochondrial-mediated cell death, enhancing the release of cytochrome c and decreasing the Bcl-2 expression, which promotes defects on transcription (Tsai et *al.,* 2004).

It is widely thought that age-related changes may be involved on MJD pathogenesis, as others neurodegenerative diseases. It is known that over decades neurons that express polyQ-containing ataxin-3 might be functional until an imbalance of cellular homeostasis that was promoted by ageing. The age-related phenomena such as activation of calpain and caspases and the decreased on chaperone activity, have been proposed to be involved on the initial steps of the disease (Barral *et al.,* 2005 and Haacke *et al.,* 2006). In fact, ataxin-3 suffers proteolytic cleavage, by calpain and caspases, forming a shortest fragment containing the polyQ tract (Haacke *et al.,* 2006). These fragments have the ability to recruit polyQ-containing proteins to aggregates, which include non-pathological ataxin-3. The incorporation of non-pathological ataxin-3 into aggregates and the corresponding reduction of soluble intracellular ataxin-3 levels could in turn contribute to MJD pathogenesis (Berke, *et al.,* 2004 and Haacke, *et al.,* 2006).

Taken together these data proposed multiple mechanisms for the implication of ataxin-3 in transcriptional dysregulation and alteration of genes expression patterns. The first one involves the interaction of mutated ataxin-3 with polyglutamine-rich nuclear factors or co-factor, like p300 and CBP. The second involves the transcriptional repression function of ataxin-3 recruiting histone deacetylase 3 and inhibiting histone acetyltransferase activity of co-activators. The third mechanism involves the effect of mutated ataxin-3 on UPP that affect the normal turnover of transcription factors.

Regardless of the existing knowledge on ataxin-3 interactions, there are still many questions to be addressed. Having this in mind, we herein present an approach for the development of a new yeast model for MJD that will ultimately allow us to increase our knowledge on the mechanisms underlying this disease.

3. Huntington's disease

Huntington's disease (HD) is a late-onset autosomal dominant disorder, characterized by neuropsychiatric symptoms, progressive loss of motor coordination and cognitive decline. In neuropathology of this disease occurs the selective dysfunction and death of specific neuronal subpopulations in the central nervous system, being gamma-aminobutyric acid (GABBA)-releasing spiny-projecting neurons, from striatum, the most affected cells. During disease progresses, there is general neuronal loss in different brain regions (reviewed in Borrell-Pagès, *et al*., 2006).

The causative gene of Huntington's disease was first assigned by Gussella and colleagues in 1983, on chromosome 4p16.3, using linkage analysis of polymorphic DNA markers of humans (Gussela *et al.,* 1983). After 10 years, Huntington Disease Research Group, using an exon amplification approach, identified a large gene, the IT15 gene, that contains in the open reading frame a polymorphic (CAG)n trinucleotide repeat tract, varying from 11 to 34 CAG in normal population (The Huntington's Disease Collaborative Research Group, 1993).

HD is caused by a mutation in the IT15 gene (HTT gene), characterized by an expansion of a variable stretch of CAG triplet in the first exon, promoting a polyglutamine-enconding tract in the N-terminal region of the huntingtin protein. Huntingtin is a 350-kDa protein characterized for the presence of different domains, including the polymorphic glutamine/proline rich domain in its amino-terminus (figure 7). This protein was observed in and outside of the nervous system. It was associated with the embryonic development, being essential for this process. In cells, it was associated with different compartments, as Golgi, endoplasmatic reticulum and mitochondria (reviewed in Landles and Bates, 2004 and Cattaneo *et al*., 2005). Specifically in neurites and synapses, this protein is associated with vesicular structures such as clathrin-coated vesicles, endosomal compartments and microtubules (reviewed in Cattaneo *et al.,* 2005).

As described for Machado-Joseph's disease, in HD the age of onset is inversely correlated with the CAG repeat length (Figure 8) and that affected individuals have more than 36 CAG repeats (Figure 9) (Duyao *et al.,* 1993).

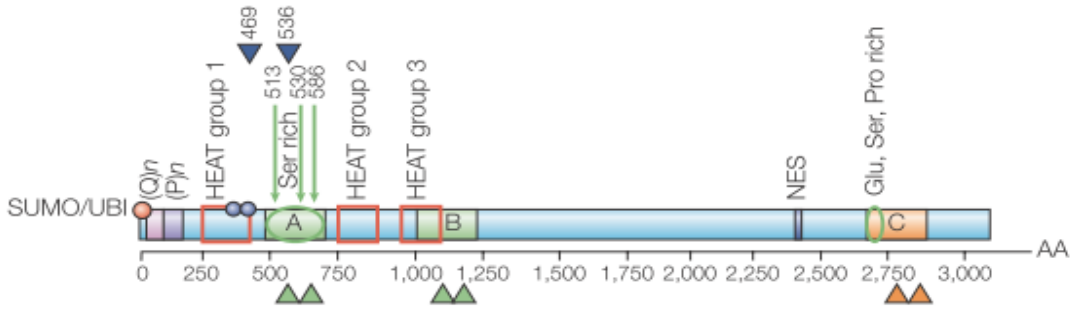

Figure 7. Schematic diagram of huntingtin amino acid sequence. $(Q)_n$ represents the polyglutamine tract; $(P)_n$ represents the polyproline sequence. The green arrows represent the caspase cleavage sites and the blue arrowheads represent the calpain cleavage sites. The green and orange arrowheads point to the approximate amino acid region for protease cleavage. The red squares represent the three main clusters of HEAT repeats. B identifies the region cleaved preferentially in the cerebral cortex, C the region mainly cleaved in striatum and A the region cleaved in both regions of brain. The red cycle indicates the post-translational modification, ubiquitilation (UBI) and/or sumoylation (SUMO) and the blue circles indicate the phosphorylation at serine 421 and serine 434. NES is the nuclearexport signal. The glutamic acid (Glu)-, serine (Ser)- and proline (P)- rich regions are indicated. (from Cattaneo *et al.,* 2005).

Several studies were performed attempting to determine the role of normal and pathogenic huntingtin in cells. It was reported that the normal and mutated protein had the ability to bind several proteins having a flexible and multifunctional structure. These abilities lead to specific conformations and different activities depending on its cellular localization (reviewed in Cattaneo *et al*., 2005). It was suggested that the neurodegeneration observed in this pathology is related to the gain of function of mutated huntingtin and the loss of function of normal huntingtin (reviewed in Landles and Bates, 2004).

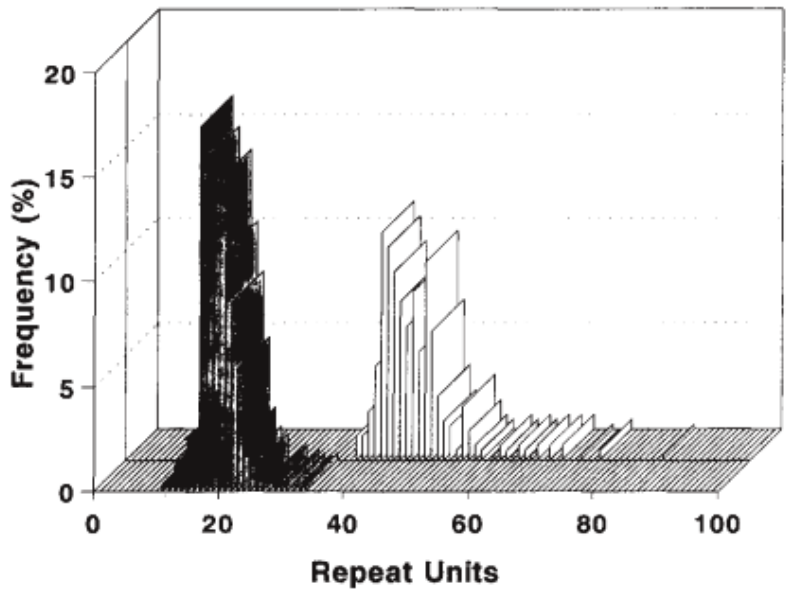

Figure 8. Comparison of CAG repeat units on control and HD chromosomes. Shaded bars, control chromosomes; open bars, HD chromosomes (from Duyao *et al.,* 1993)**.**

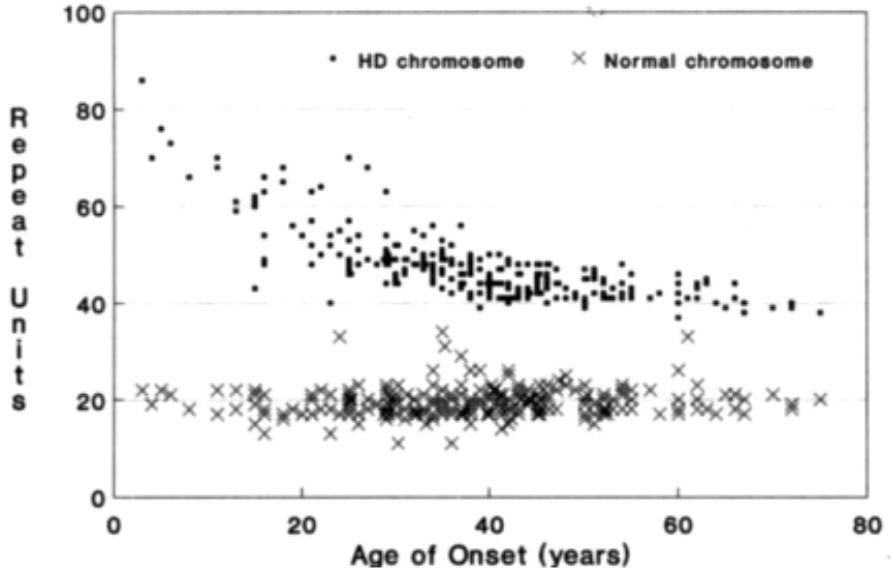

Figure 9. Relationship between repeat unit length and age of onset (from Duyao *et al.,* 1993).

As described for others polyQ disorders, such as Machado-Joseph's disease, huntingtin protein also suffers proteolytic cleavage, resulting a fragment containing the first exon of HTT gene. These fragments were described as being more toxic than the full-length protein. Moreover, huntingtin flanking sequences and its protein interactions also determines its toxicity (Duennwald *et al.,* 2006a and Duennwald *et al.,* 2006b). Huntingtin was found in the nucleus of specific brain regions. Nevertheless, this protein lacks the classic importin beta-dependent polypeptide sequence, the nuclear localization sequence (NLS), to enter to nucleus. Were then hypothesized that polyglutamine tract has NLS activity or huntingtin has high affinity to NLS-containing protein, such as transcription factors, forming complex that allow its import into the nucleus (reviewed in Truant 2003 and Truant *et al*. 2006). The full-length protein has a nuclear export sequence (NES) (Figure 7) that is not present in the huntingtin fragment leading to a highest toxicity of the fragment compared to full-length huntingtin. The fragment toxicity was related to the capacity of the protein to bind several proteins and its nucleocytoplasmic transport (Figure 10) (reviewed in Truant 2003).

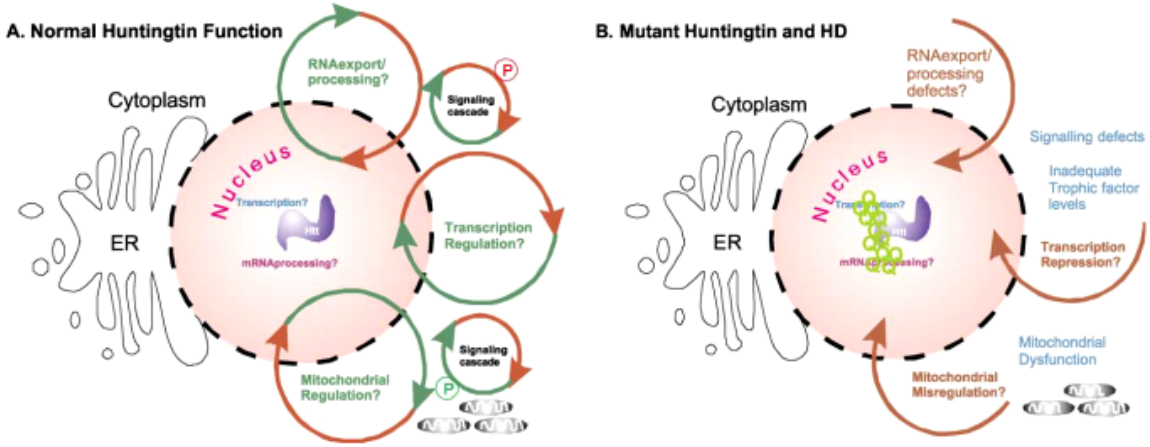

Figure 10. Potential biological roles of huntingtin protein in nucleocytoplasmic transport. Huntingtin interacts with diverse proteins involved on transcription, trafficking and endocytosis, signaling and metabolism processes (from Truant 2003).

In attempt to dissect the role of huntingtin fragment in the disease, Rockabrand and colleagues found that the first 17 amino acids of exon 1 are involved in the huntingtin fragment association with cytosolic organelles, such as mitochondria and ER (Rockabrand *et al.*, 2007). Furthermore these amino acids when mutated enhance the propensity of fragment to aggregate (Atwal *et al.*, 2007 and Rockabrand *et al.*, 2007) and also may be involved in the disruption of [Ca^{2+}] homeostasis (Rockabrand *et al.*, 2007). Towards the understanding of the effects of the first amino acid sequences of huntingtin, Atwal and colleagues, observe that this region, that are well conserved in all vertebrate species, may be involved in huntingtin sub-cellular localization, having a membrane targeting domain that can mediate the association of huntingtin with the ER. When the association of huntingtin/ER is disrupted, by point mutations, was observed the capacity of huntingtin to enter in the nucleus. With these observations the authors suggest that polyglutamine expansion may inhibit proper ER-targeting or nuclear shuttling of huntingtin leading to increased protein levels in the nucleus (Atwal *et al.*, 2007).

Using a yeast model, Solans and colleagues demonstrated that the expression of a mutant fragment of huntingtin (first exon) affects the mitochondrial homeostasis soon after large SDS-insoluble aggregate start to form (Solans *et al*., 2006). They described that this fragment impairs the OXPHOS complex II+III activities, leading to deficits in respiratory capacity and leading to an increased production of free radicals. They also observed that the distribution and morphology of the mitochondrial network are progressively disturbed and may be the result of the disruption of actin cytoskeleton (Solans *et al*., 2006). These data support the idea that mutant hintingtin toxicity was associated with the apoptotic process (Leavitt *et al*., 2001) and that wild-type huntingtin can reduce the apoptotic toxicity of mutant huntingtin, suggesting that wild-type protein may normally have an anti-apoptotic function (Leavitt *et al*., 2001). Moreover, Zhai and colleagues, using an in vitro transcription assay with different huntingtin N-terminal fragments, demonstrate that several components from transcription machinery are target by mutant huntingtin. Also, it was demonstrated that soluble form os mutant huntingtin directly dysregulate transcription interfering with specific components, such as TFIID and TFIIF (Zhai *et al.*, 2005). The mutant huntingtin is also associated with inhibition in the production of BNF (Brain-derived neurotrophic factor).

Wild-type huntingtin bind repressor element-1 silencing transcription factor/neuron restrictive silencer factor (REST/NRSF), sequester this transcription repressor in cytosol promoting the expression of BDNF (brain-derived neurotrophic factor), important for the survival of striatal neurons. In HD this mechanism is affected, the mutant huntingtin had reduced capacity to bind REST/NSRF lead to their entrance to nucleus and repress the expression of BDNF (reviewed in Truant *et al*., 2006).

As in others polyglutamine diseases, in HD a role on UPP has been demonstrated. Using cellular and trangenic mouse models, it was demonstrate that the proteasome is involved in degradation of polyglutamine-expanded truncated N-terminal huntingtin and that the rate of degradation was inversely dependent on glutamine-repeat length (Jana *et al.,* 2001). Moreover, it was shown that altered proteasome activity is associated to the disruption of mitochondrial membrane potential, leading to the release of cytochrome c into cytosol and activation of caspase3- and caspase 9-, culminate in to apoptotic cell death process (Jana *et al.,* 2001). The impairment of proteasome activity has also been reported to induce the expression of several cytoplasmatic heat-shock proteins and ER-resident chaperones (Cowan et al., 2003 and Jana *et al.,* 2001).

The data here reported lead us to raise new questions on the mechanisms underlying the disease. Having this in mind, we herein present new insights on the role of autophagy in HD disease.

4. Models for study neurodegenerative disorders

A growing number of completed sequencing genomes have revealed that the sequence information *per se* is highly uninformative. Nevertheless, the determination of the pathogenesis of diseases is not only based in the basic units of information, the genes, but involves more complex systems (van Ham *et al.*, 2009). To understand the systems involving the disease pathogenesis, different models can be used. To develop a model for studying the different neurodegenerative diseases must be taken into account the proposal question and answers that we want to address. Until now several models were being used

to dissect the neurodegenerative diseases pathogenesis (Table II). The different models used were described in the next sections.

Table II. Conservation of genetics of human disease in models used to protein aggregation research (from van Ham *et al.*, 2009).

	Proteins encoded in genome	Human disease gene orthologues (nr)
Yeast (*Saccharomyces cerevisiae*)	6241	290
Worm (*Caenorhabditis elegans*)	18,424	533
Fruit fly (*Drosophila melanogaster*)	13,601	724
Mouse (*Mus musculus*)	26,258	1354
Human (*Homo sapiens*)	20,000–25,000	n.a.

'Proteins encoded in genome' indicates the estimated number of proteins encoded by the genome; for yeast, *C. elegans* and *Drosophila* the estimations from Rubin et al (2000) were used, for mouse, the Mouse Genome Informatics from Jackson Laboratory (jax.bioinformatics.org; September 2009), and for human the estimation from the International Genome Sequencing Consortium. The human disease homology indicates the number of genetic orthologue clusters to human disease genes, relating to the number of orthologues in that model organism of human disease genes, a measure for the genetic conservation of human disease genes (O'Brien et al, 2004, Human Mutation; http://orthodisease.cgb.ki.se).

4.1. Mammal models

Mouse and cell cultures were the most commonly used models, to complement clinical study of these disorders, due to their complexity and simplicity, respectively.

In mouse case, it is possible to use transgenic or knock-in mouse models to further provide new valuable insights into the mechanisms associated with the development of the diseases, particularly the early changes and into preclinical testing of therapeutic strategies (reviewed in Rubinstein, 2002). These models also permit an in-depth analysis of the different stages of the disease process and are helpful to identify the factors related to the somatic repeat instability (reviewed in Bates and Davies, 1997). In long term both models will be required to test candidate drugs designed to prevent or interrupt the disease process.

Although these models will be invaluable in developing or understanding of the molecular pathways by which a polyQ tract can cause cell death (reviewed in Bates and Davies, 1997).

4.2. Invertebrate models

The invertebrate models encompass the *Drosophila melanogaster* and *Caenorhabditis elegans* organisms (Brignull *et al*., 2006), being one of the classical tools used for unbiased genetic screens in several neurodegenerative disease studies (Table III).

Drosophila melanogaster has been used as a model for investigating complex biological processes, that are common with humans, such as regulation of gene expression, membrane trafficking, cell signaling and cell death (Sang and Jackson, 2005 and Guo, 2010). This model has a compact genome ($1/30^{th}$ of human genome), limited genetic redundancy, and a short generation time (10 days). The sequencing genome has revealed that 77% of human disease genes are conserved in the fly (Guo, 2010) and has several cellular pathways shared with humans (van Ham *et al*., 2009). Furthermore an availability of a number of genetic manipulations that are impossible or impractical to carry out on mammals is possible to perform in this model.

It was used the fly eye, as a model, given that the adult eye phenotype are easy to detect. Moreover, the eye is tolerant to genetic disruption of basic biological processes and under laboratory conditions it is necessary to fly survival (Sang and Jackson, 2005). Using the fly eye is possible study the cell control, cell proliferation and differentiation, neuronal connectivity (Link, 2001) and the processes involving cell death and age-associated neurodegeneration (Sang and Jackson, 2005).

The potential of the screens performed using *Drosophila* model has stimulate the development of other invertebrate models as *C. elegans*. *C. elegans* model has sufficient complexity and simplicity to allow investigation of cellular and behavioral phenotypes which facilitates the high-throughput testing of hypotheses (Brignull *et al.,* 2006). The invertebrate models should be viewed as genetic systems that allow the isolation of

modifiers genes or the screens of libraries at a speed that might be difficult if not impossible to accomplish in mammalian models (Link, 2001)

Although, these models show late-onset and progressive pathology, not been possible directly address the age-associate nature of the neurodegenerative disease (Link, 2001).

Table III. Description of several studies using invertebrate models to dissect the role of polyQ disease related-proteins (adapted from Link, 2001).

Protein expressed (transgenic model)	Expression pattern	Associated phenotype?	Transgenic protein aggregation?	Initial reference
Polyglutamine repeat diseases				
Truncated SCA3/MJD, 27 or 78 Q (*Drosophila*)	Eye, pan-neuronal, mesodermal, *dpp*	Range from subtle eye abnormality to lethality	Nuclear inclusions	Warrick et al. (1998)
N-Terminal huntingtin, 2, 75, or 120 Q (*Drosophila*)	Eye	Eye cell degeneration	Nuclear inclusions	Jackson et al. (1998)
N-Terminal huntingtin, 2, 23, 95, or 150 Q (*C. elegans*)	Sensory neurons	Neurodegeneration	Cytoplasmic aggregates	Faber et al. (1999)
PolyQ only, polyQ epitope-tagged, Dsh::polyQ, 22 or 108 Q (*Drosophila*)	Eye, pan-neuronal. *Dpp*	Eye abnormality to lethality	Nuclear and cytoplasmic inclusions	Marsh et al. (2000)
PolyQ epitope-tagged, 20 or 127 polyQ (*Drosophila*)	Eye	Eye abnormality	Nuclear inclusions	Kazemi-Esfarjani and Benzer (2000)
GFP::polyQ, 19 or 82 Q (*C. elegans*)	Body wall muscle	Slow growth	Cytoplasmic	Satyal et al. (2000)

4.3. Yeast models (Nervous Yeasts)

Several studies were performed using yeast as a model to study neurodegenerative diseases (Duennwald, *et al*., 2006a; Duennwald, *et al*., 2006b and Outeiro and Linquist, 2003). *Saccharomyces cerevisiae* was the first eukaryote organism to be fully sequenced in 1996 (Goffeau *et al.,* 1996). After 14 years about 80% of the proteins predicted to be encoded in the yeast genome have been characterized functionally. Furthermore, the yeast research community built valuable biological tools to work with this model (Table IV) and the data obtained from different genomic approaches are well organized and actualized in public databases (reviewed in Tenreiro and Outeiro, 2010).

Table IV. Some examples of the yeast collection available for genetic screens (from Tenreiro and Outeiro, 2010).

Collection	Type	Source/reference
Yeast haploid and diploid deletion strains	Strains with individual genes replaced by the KanMX4 cassette	Winzeler *et al.* (1999)
Yeast-GFP clone collection	Genome insertions	Huh *et al.* (2003)
Yeast GST-fusion Collection	Vector library	Martzen *et al.* (1999)
Yeast-TAP fusion library	Genome insertions	Ghaemmaghami *et al.* (2003)
Yeast Tet-promoters – yTHC	Promoter-shutoff strains for essential yeast genes	Mnaimneh *et al.* (2004)
TRIPLES	Yeast transposon insertion library	Kumar *et al.* (2002)
Yeast promoter library constructed in a vector containing two reporter genes (EGFP and lacZ)	Vector library	Bell *et al.* (1999)

Yeast models have been instrumental for our current understanding of conserved cellular mechanisms such as cell division, the DNA replication, the metabolism, the protein folding and the intracellular transport. Moreover, this model express numerous genes with human orthologs that can be rapidly manipulated using established genetic techniques (reviewed in Chen *et al* 2005).

The yeast model is widely used to understand the molecular mechanisms involved in different neurodegenerative diseases, because it is known that the basic mechanisms and pathways involved in these processes are highly conserved between yeasts and humans, such as mitochondrial dysfunction, transcriptional dysregulation, trafficking defects and proteasomal impairment (Figure 11) (Winderickx et al., 2008 and reviewed in Tenreiro and Outeiro, 2010). Moreover, there others advantages in using this model as the reduced complexity of yeasts compared to neurons and the all the cDNA libraries available to study the mechanism behind the disease. Nevertheless, such as others models yeast cells have some limitations. Yeasts compared to neurons are not embedded in tissues neither functionally linked to other cells, and lack the neuron-specific morphological structures, such as dendrites, axons and synapses. Specially compared to neurons, yeasts have a less diverse collection of molecular players, nevertheless the basic molecular process were conserved between neurons and yeasts (reviewed in Braun *et al.,* 2009). The high similarity of same mechanisms makes possible the modulation of molecular mechanisms

in yeasts cells using the genetic and postgenomic tools, such as collections of strains and plasmids, enable to identify novel modifiers of aggregation and toxicity, which are central hallmarks of these diseases (reviewed in Tenreiro and Outeiro, 2010). Furthermore the yeast models are also being implicated in drug discovery efforts.

In yeasts there are two different approaches to study the human neurodegenerative diseases. If the gene implicated in the disease has a yeast homolog, it is possible to study its function directly. If, on the other hand, the gene underlying the disease is absent in yeast genome, it can be modeled by the heterologous expression of the human gene in yeast cells. Nevertheless, the results obtained in yeast models need to be confirmed in other *in vitro* and *in vivo* models, such as neuronal cells, worms or flies to validate the putative targets for therapeutic intervention (Figure 12) (reviewed in Tenreiro and Outeiro, 2010).

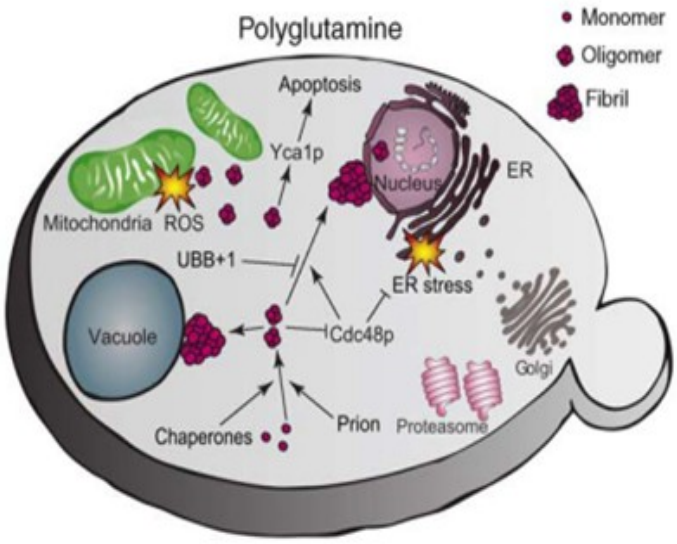

Figure 11. Yeast model for Polyglutamine diseases (from Braun *et al.,* 2009).

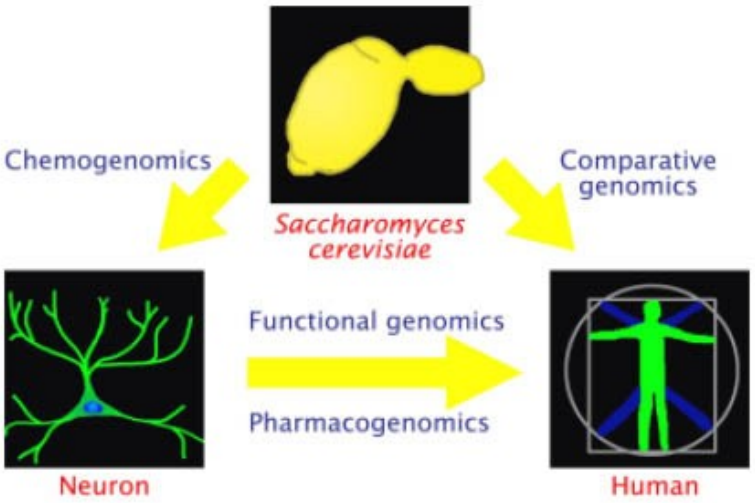

Figure 12. Schematic representation of yeast *Saccharomyces cerevisiae* being a eukaryotic model in combination with other cell and animal models (from Tenreiro and Outeiro, 2010).

4.3.1 Yeast and Aging process

Aging is an important factor to develop neurodegenerative diseases and yeasts are a widely used model for study the cellular aging. Using this model is possible to study the mechanism associated to aged diseases through two mechanisms, the replicative life span (RLS) and the chronological life span (CLS or chronological aging) (Figure 13). The RLS was defined as the number of dougther cells produced by a mother cell before senescence and the CLS, which was recently developed in yeast, is defined as the length of time a population maintains viable in a nondividing state (stationary phase), mimicking the situation of postmitotic cells, such neurons (Figure 13). These two models of aging provide a unique opportunity to compare the aging processes of both proliferating and nonproliferating cells in (reviewed in Braun *et al.,* 2009; Chen *et al.,* 2005 and Kaeberlein *et al.*, 2007).

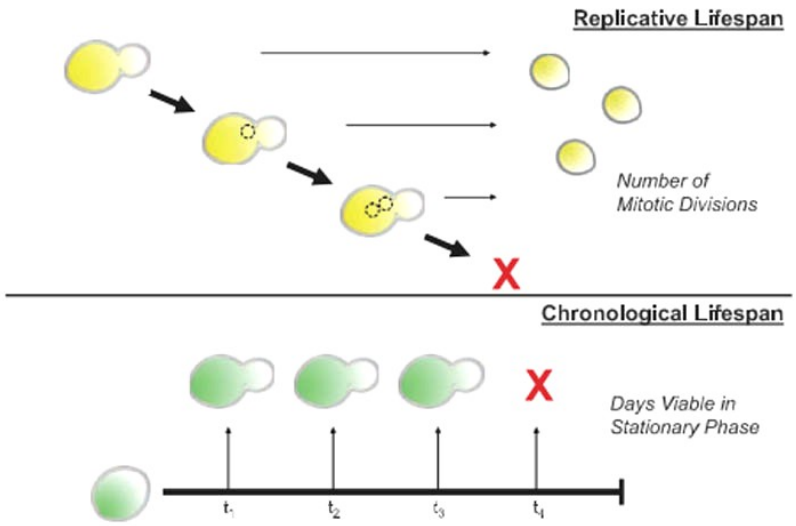

Figure 13. Schematic representation of yeast replicative and chronological life span (from Kaeberlein *et al.*, 2007).

5. Autophagy, proteasome and aging on polyglutamine diseases

5.1. Autophagic process

Autophagic process was described more than 50 years ago, but only in the past decade the molecular basis were elucidated, achieved through genetic approaches in yeast mutants defective in autophagy (reviewed in Kundu and Thompson, 2008).

Autophagy is a cellular process in which cellular components are sequestered in double membrane vesicles and delivered to lysosome for degradation and recycling of bioenergrtic components (reviewed in Kundu and Thompson, 2008). This process is extremely well regulated and it is involved in turnover of long-lived proteins and in the elimination of supernumerary or damage organelles, such as mitochondria and ER (reviewed in Maiuri *et al.,* 2007). Moreover, autophagy is a process that represents a single cell adaptation to starvation. Through catabolism of macromolecules, autophagy

generates metabolic substrates to provide bioenergetics components to cells and thereby allows the adaptative protein synthesis (reviewed in Maiuri *et al.,* 2007 and Mizushima *et al*., 2008).

The basic steps and the molecular machinery involved in autophagy are conserved between yeasts and humans (reviewed in Kundu and Thompson, 2008). There are seven well described steps in the autophagic process (reviewed in Kundu and Thompson, 2008). The initiation process includes induction or selection/packaging of cargo, depending of the activated pathway, if the stimuli promote the activation of selective or nonselective pathways. Subsequent steps include nucleation, vesicle expansion, completion, fusion, degradation and export of metabolic components (Figure 14-A) (reviewed in Kundu and Thompson, 2008).

Autophagy is induced when cells enters in starvation, where the target of rapamycin (TOR) kinase is inactive. Nevertheless, there are others pathways that lead to a autophagy induction. The basal levels of autophagy are important for maintain normal cellular homeostasis. The TOR regulates the switch between autophagy (Figure 14-B) and the cytoplasm-to-vacuole targeting (CTV) pathway, changing the interaction between serine-threonine kinase *ATG1* with other components of the induction complex, including *ATG13*, *ATG17* and *ATG11* (reviewed in Høyer-Hansen and Jäättelã, 2007 and Kundu and Thompson, 2008).

When autophagic process is activated, specific autophagic proteins are recruited leading to the formation of the double membrane autophagosomes, contain cargo proteins or organelles, such as mitochondria, ER and peroxisomes, which will dock and fuses with lysosomal (mammals)/vacuolar membrane (yeasts) and starts the degradation process (reviewed in Kundu and Thompson, 2008). Finally, the bioenergetic components resulting from degradation are exported from lysosome/vacuole (reviewed in Kundu and Thompson, 2008). Yeast genome presents more than 30 autophagy-related (*ATG*) genes involved in autophagic process were identified in yeast cells. Some of them participate in all types of autophagy while others only participate on one or few particular types of autophagy (Figure 14-B) (reviewed in Kraft *et al*., 2009).

Some studies suggest that the apoptotic and the autophagic processes inhibit each other. If the apoptotic machinery is inhibited there is a switch response to an increased in

the autophagy. The autophagic process has a dual ellefct on cells, can act as cytoprotective process or a cellular death process (reviewed in Maiuri *et al.,* 2007).

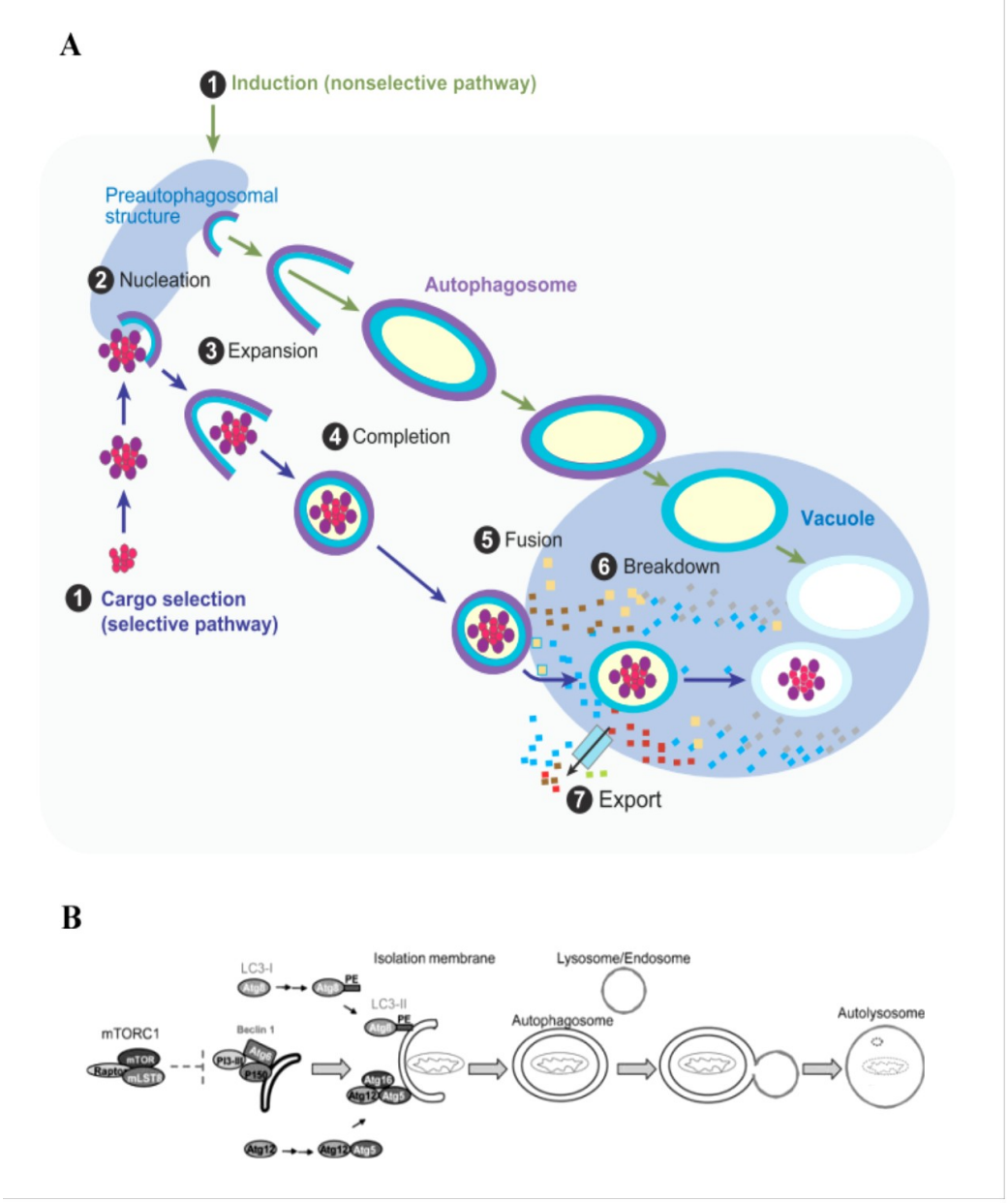

Figure 14. A) Schematic representation of autophagic process. The signal to initiate the autophagy comes from nonselective pathway, relative to changes in nutrient availability, or selective pathway, relative to cargo proteins or organelles (from Kundu and Thompson, 2008). B) Schematic representation of autophagic regulation (from Høyer-Hansen and Jäättelã, 2007).

The involvement of autophagy in cellular suicide may be explained by the direct self-destruction of massive autophagy or, alternatively, by hardwiring of the autophagic process to pro-apoptotic signal (reviewed in Maiuri *et al.,* 2007).

There are two major degradation pathways in cells, the ubiquitin proteasome pathway (UPP) and autophagy.

The ubiquiton proteasome pathway (UPP) is responsible for the degradation of short-lived proteins. In this pathway proteins are ubiquitilated and then shuttled to 26S proteasome. The 26S proteasome is a multimeric structure composed of a 20S core subunit, with four rings, capped by two 19S regulatory subunits. The proteolytic degradation of ubiquitilated proteins takes place within the 20S core subunit following removal of the ubiquitin monomers by deubiquitination enzymes (DUB) and folding of the substrate protein (reviewed in Lehman, 2009).

Ding and colleagues, using transfected cells, observed a relation between autophagy and UPP (Ding *et al.,* 2007). They demonstrated that if the UPP is inhibited then there is an activation of autophagy. When an impairment of the UPP occurs there is an accumulation of polyubiquitinated proteins that causes the accumulation of misfolded proteins in the ER, leading to ER stress. In this situation seems that autophagy is activated to compensate the UPP impairment and ameliorates de ER stress (Ding *et al.,* 2007). With these studies it was demonstrate that diverse pathways may be involved on relation between autophagy and UPP.

5.2. Autophagy, aging and neurodegenerative diseases

Growing evidences point a role for autophagy in diverse human diseases, such as in neurodegeneration, cancer, infection and immunity, heart disease, myopaties and liver diseases (Mizhushima *et al.,* 2008). There are several antibiotics that block or enhance the autophagic process, as shown in figure 15 that contributed to the understanding of the effects of autophagy in neurodegenerative and other diseases (reviewed in Maiuri *et al.,* 2007).

Among these antibiotics, one of the best described is rapamycin. This substance is an enhancer of autophagy (figura 15) by inhibiting the mTOR pathway leading to the induction of autophagy. Several studies were performed using this enhancer in order to understand its effect on neurodegeneration. More recently, Pan and colleagues, using PC12 cell line with proteasomal dysfunction, induced by lactacystin, and C57BL/6 mice, demonstrated that these cells presents neuronal death with formation of α-synuclein of ubiquitin-positive cytoplasmatic inclusion and inducing autophagy (Pan *et al.,* 2008). When cells were treated with rapamycin, the lactacystin-induced apoptosis was attenuated and cells were rescued from lactacystin induced loss of dopaminergic neurons (Pan *et al.,* 2008).

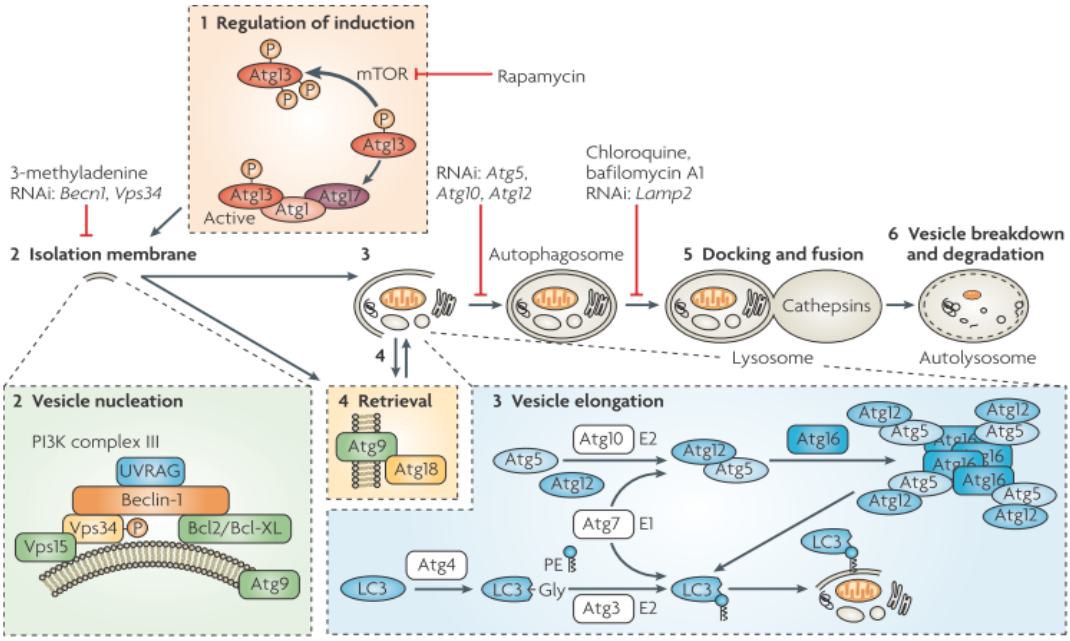

Figure 15. Schematic representations of autophagy and its inhibitors (from Maiuri *et al* 2007).

In mouse model of Machado-Joseph disease it was shown that the induction of autophagy leads to a reduction on mutant ataxin-3 levels (Menzies *et al.,* 2010). Furthermore, in *Caenorhabditis elegans* model, using a siRNA to knock down autophagy-related genes, it was shown an increase of aggregate-containing cells and that this aggregates were focus on nucleus (Khan *et al.,* 2008).

These, as well as others studies, indicate that the induction of autophagy has a neuroprotective role, when the ubiquitin-proteasome was impaired (Pan *et al.,* 2008). Taken together these studies reveal a close kink between autophagy and neurodegeneration. Moreover, these processes are related with aging process.

There is an accumulation of damage proteins and damage organelles with age, caused by different factors, such genetic factors, environmental influences and certain diseases (Figure 16) (reviewed in Vellai, 2009), leading to an imbalance between the rate of protein damage and protein turnover. The accumulation of damage organelles or structures lead to the reduction of cellular efficiency of biological processes that are required to maintain homeostasis and survival, which could contribute to aging process (reviewed in Cuervo *et al.*, 2005 and Rajawat and Bossis, 2010). Nevertheless, the precise mechanism of aging is not yet completely understood.

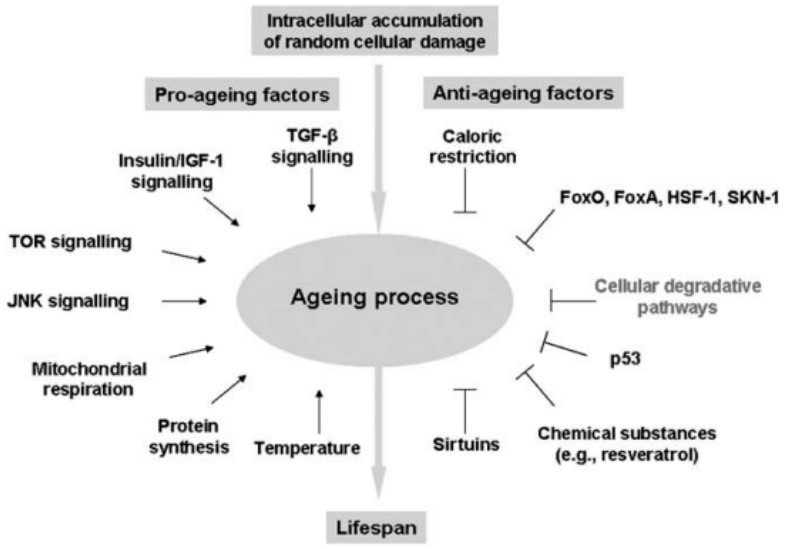

Figure 16. Environmental clues and evolutionary conserved pathways that regulate the aging process in diverse eukaryotic phyla (from Vellai, 2009).

Lysosomes have a pivotal role on aging. Age-related alterations of lysosomal system leads to the accumulation of lipofuscin (pigmented product) as a result of incomplete digestion of engulf components (reviewed in Cuervo, 2008 and Rajawat and Bossis, 2010). The rate of lipofuscin formation is inversely related to age, and lysosomes with lipofuscin have a reduced ability to fuse with autophagic structures. Mitotic cells can eliminate lipofuscin by diluting the pigment in each mitotic cycle. However pos-mitotic cells, like neurons, do not have this ability (reviewed in Cuervo, 2008 and Rajawat and Bossis, 2010). Lipofuscin, thus, seems to be an important contributor to cellular degeneration, and not only a hallmark of aging (reviewed in Cuervo *et al.*, 2005). Furthermore macroautophagy dysregulation in old organisms could also be a consequence of its persistent activation as demonstrated in rodent liver (reviewed in Cuervo, 2008).

An important limitation of the studies linking autophagy and aging is that autophagy blockage is induced early in life (invertebrates and mammalian models), whereas the age-dependent decrease in this pathway does not begin in most organisms until middle age (reviewed in Cuervo, 2008). Further studies, using yeasts as a model, should be done take this limitation in account.

6. Objectives

The general goal of the studies described in this thesis is to improve the knowledge on polyglutamine expansion diseases, using a yeast model.

The first goal of this study was the development of yeast model for Machado-Joseph disease (MJD) with variants 1 and 2 genes under the control of Tet On system.

The second goal was the characterization of the yeast model for Huntington's disease (HD). For the characterization of Huntington's model we want to address the effect of autophagy on the pathogenesis. For this purpose, we used chloroquine to inhibit the autophagic process in cells expressing normal and mutated huntingtin protein at exponential, diauxic and stationary phase of yeast life cycle.

II. Materials and Methods

II. Materials and Methods

1. Construction Machado-Joseph disease models

1.1 Construction of ATXN3 variants on pUG35 plasmid

1.1.1 DNA manipulations and Cloning

The ATXN3 variants, 1-1, 1-1E, 2-1 and 2-1E were obtained from plasmidic DNA, pCMV and pEGFP-C, respectively, kindly provided by Dra. Patrícia Maciel (ECS/ICVS-UM) via PCR amplification using the primers 1 and 2 or 3 (Results, Table I) that included, respectively, *Bam*HI and *Hind*III restriction site for cloning into the pUG35 plasmid, which will allow the genes fusion with GFP. To amplify the fragments, 200 ng of DNA were added to 49.5 µl of reaction mixture defined by reaction buffer 1x with 1.5 mM $MgCl_2$, 0.2 mM dNTP, 1 mM of each primer and 2.5 units High Fidelity PCR enzyme (Fermentas), the PCR amplification was performed on My Cycler™ (Bio-Rad) following the condition described in Table II (Results). The fragments were extracted from a 0.8% agarose gel prepared on TAE buffer (40 mM Tris-Base, 2 mM EDTA, Glacial Acetic Acid to pH 0.8) and purified gel using Silica Bead DNA Gel Extraction Kit (Fermentas). The amplified fragments and plasmid was digested using the referred restriction enzymes, *Bam*HI and a *Hind*III (Fast Digest enzyme, Fermentas) during 3hours. Followed by new products purification, performed with Silica Bead DNA Gel Extraction Kit (Fermentas), afterwards the products were run in a 0.8% agarose gel and extracted from the gel. The purified products were then quantified on NanoDrop® ND-1000 Spectrophotometer (Alfagene). To perform the ligation between gene fragments and linear plasmids was used 2 units of T4 DNA Ligase (Fermentas), during 1 hour at 26ºC. The products resulting from ligation reaction were transformed in E*scherichia coli*, using the Inoue Method. Briefly, ~25ng of ligation product DNA were added to 90µl of competent *E.coli* cells, which were then submitted to 30 minutes incubation on ice, followed by the heat shock during 45 seconds at 42ºC and incubation on ice for 10 minutes. Afterwards, to the mix were added 800 µl of SOC (Super Optimal broth with catabolite repression) medium and incubated during1 hour, at 37ºC with 250 rpm shaking. After the recovery in SOC medium (2% Tryptone,

0.5% Yeast extract, 0.05% NaCl, 0.0186% KCl, at pH 6.7) the cells are centrifuged for 1 minute at 13,000 rpm, ressuspended in 100 µl of SOC medium and plated in LB amplicillin medium (Sambrook and Russell, 1989).

1.1.2 Analysis of transformants

The plasmid isolation was performed on overnight cultures by Fast Alkaline Lysis. Therefore 3 ml of LB ampicillin liquid medium with the bacterial cells were centrifuged and resuspended in 250 µl of resuspension buffer, followed by the addition of 250 µl of Solution 2 (1% SDS and 200 mM NaOH), after 5 minutes it was added 300 µl of Solution 3 (3 mM Potassium acetate). The Mix was centrifuged and it was added 600 µl of Isoporanol (100%) to perform the DNA precipitation. To carry out the DNA wash, 200 µl of 70% Ethanol were added to the pellet. After ethanol evaporation, the DNA was resuspended in 50 µl of TE buffer (1 mM EDTA, 10 mM Tris-HCl, pH 8.0) with 10 µg/ml RNase A. The plasmidic DNA of transformants was analyzed for the introduction of the variant genes by restriction digestion analysis. The pUG35::ATXN3 variant genes were digested with *Bam*HI and *Kpn*I, or only *Kpn*I, and with *Eco*RI and *Eco*RV during 3 hours. The resultant digested products were run in 0.8% agarose gel.

1.2 Construction of ATXN3-GFP variants on pCM252 plasmid

1.2.1 DNA manipulations and Cloning

The ATXN3 variants, 1-1, 1-1E, 2-1 and 2-1E fused with GFP were obtained from pUG35 plasmidic DNA, described in the precious section, via PCR amplification using the primers 1 and 4 (Results, Table I) that included, respectively, a *Bam*HI and a *Apa*I restriction site for cloning into the pCM252 plasmid. To amplify the fragments, 200 ng of DNA were added to 49.5 µl of reaction mixture defined by reaction buffer 1x with 1.5mM

$MgCl_2$, 0.2 mM dNTP, 1 mM of each primer and 2.5 units High Fidelity PCR enzyme (Fermentas), the PCR amplification was performed on My Cycler™ (Bio-Rad), following the condition described in Table III (Results). The resultant fragments were extracted from a 0.8% agarose gel prepared on TAE buffer (40 mM Tris-Base, 2 mM EDTA, Glacial Acetic Acid to pH 0.8) and purified using Silica Bead DNA Gel Extraction Kit (Fermentas). The amplified fragments and plasmid were digested using the referred restriction enzymes, *Bam*HI and *Apa*I (Fast Digest enzyme, Fermentas) during 3hours. The ligation and transformation conditions were the same described above in the section **1.1.1**.

1.2.2 Analysis of transformants

The plasmid extractions were performed as described in the section **1.1.2.** Plasmidic DNA of transformants was analyzed for the introduction of the variant genes fused with GFP by restriction digestion analysis. The pUG35::ATXN3-GFP variant genes were digested with *Bam*HI or *Apa*I during 3 hours. The resultant digested products were run in 0.8% agarose gel.

2. Studies on yeast model of Huntington's disease

2.1 Strains, media and treatments

In this study it was used the *Saccharomyces cerevisiae* wild-type strain W303-1a (MAT*a*; ura3-52; trp1Δ 2; leu2-3,112; his3-11; ade2-1) harboring pCM252 plasmids with exon 1 fragment of IT15 gene (gene associated to Huntington's disease) with 25 CAG and 103 CAG, this fragments were C-terminally tagged with *GFP* gene (kindly provided by Dr. Fulvio Reggiori). All yeast cultures were inoculated in selective YNB medium, containing 0.67 % (w/v) Yeast Nitrogen Base (Difco Laboratories), 2% (w/v) glucose as carbon source, supplemented with the appropriate amino acids: 100 µg/L uracil, 300 µg/L

leucine, 50 µg/L histidine and 100 µg/L adenine. All cultures were grown overnight at 26°C, with shacking at 150 rpm. Cells were collected at early exponential, late exponential (diauxic) and stationary phases and doxycycline (2 µg/µl, Sigma) was added to the growth medium. Growth was monitorized (each 2 hours) by measuring the turbidity of the culture at 640 nm in a 'Spectronic Genesys 20' spectrophotometer (Thermo Spectronic). To assess the effect of inhibition of autophagy on cells expressing the disease-related genes was added to the medium choloroquine (50µg/µl, Sigma), at the same time points at which was induced the protein expression.

For determination of cell survival, cellular samples were serially diluted and platted on YEPD agar plates, consisting in 0.5 % (w/v) yeast extract (Difco Laboratories), 1% (w/v) peptone (Difco Laboratories), 2% (w/v) glucose and 2% (w/v) agar, until the culture reach an 0.1% of cell survival. The viability was determined by counting colony-forming units (CFUs) after 2 days of incubation at 30°C. The CFUs on time 0 (when doxycycline was added to the culture medium) were counted as 100% survival.

2.2 Epifluorescent Microscopy

Images were acquired in an Olympus BX61 (Olympus, United States) microscope with filter wheels, to control excitation and emission wavelengths, equipped with a high-resolution DP70 digital camera and using an Olympus UPlanSApo 100X/oil objective, with a numerical aperture of 1.40. All the samples were suspended in PBS and Vectashield® (Vector Laboratories, Burlingame, Canada) and visualized at room temperature.

2.3 Preparation of total protein extracts and Western Blot Analysis

For detection of protein levels by western-blot, the total cellular extracts were collected at the specific time points and disrupted using glass beads in lysis buffer (1%

(v/v) Triton X-100, 120 mM NaCl, 50 mM Tris-HCl pH 7.4, 2 mM EDTA, 10% (v/v) Glycerol, 1 mM PMSF and Complete Mini protease inhibitor cocktail (Roche, Mannheim,

Germany). 40 µg of total protein were resolved on a 12% SDS gel and transferred to a nitrocellulose membrane during 90 min at 100V. Membranes were blocked with phosphate-buffered saline (TBS) with 0.1% Tween 20 (TBST) containing 5% skim milk, followed by incubation with rabbit anti-GFP (Invitrogen) primary antibody (1:10000) an with conjugated anti-rabbit IgG secondary antibody (Cell Signaling) (1:5000) and detected by enhanced chemiluminescence.

2.4 Statistical analysis

The results shown are mean value and standard deviations of at least three independent assays.

III. Results

1. Development of a yeast model for Machado-Joseph's disease

In the last decade several yeast models were developed to study and characterize the neurodegenerative disease-related proteins. Despite the fact that yeast cells are not embedded in tissues neither functionally linked to other cells, and lack the neuron-specific morphological structure, they have already proved to be a valuable model for the study of basic molecular aspects of several human neurodegenerative diseases, such as Huntington disease (HD), a polyQ disorder (reviewed in Braun *et al*., 2009). PolyQ disorders are characterized by the presence of a CAG tract on causative gene, resulting in a protein with a poly-glutamine tract (Kawaguchi *et al*, 1994 and Cattaneo *et al.,* 2005). These proteins are prone to misfold and form aggregates which might have different negative effects on cellular physiology (Gao and Hu, 2008).

HD is the most studied polyQ disorder and the findings obtained in the study of this disease are tempting to be extrapolated to other polyQ disorders. Nevertheless, in the last years, a number of reports have suggested that each polyQ disorder has specificities and special care should be taken when generalizing the data obtained in HD (Ross *et al.,* 1999). Taken this into consideration, we decided to develop a new yeast model for Machado-Joseph's disease (MJD) that has never been described. The yeast *Saccharomyces cerevisiae* due to the powerful available genetic resources and the accumulated knowledge in the field has enlarged its importance as a model for several neurodegenerative diseases (Tenreiro and Outeiro, 2010). Two different strategies can be adopted to develop yeast models. If a gene implicated in the disease in study has an homologous in yeast, its function is directly study, while, if the gene is absent, it can be studied by its heterologous expression in yeast cells. Therefore, like in other yeast models, such as Parkinson or Huntington, the MJD models were developed based on the hererologous expression of the human disease-related genes, Ataxin-3 (ATXN3) with different polyQ tracts. For the construction of the MJD models two ATXN3 variants were used, taking into account that the vast majority of the studies in different models used the selected variants: (i) MJD1-1 variant carrying a tract $(CAG)_2CAAAAGCAGCAA(CAG)_8$ coding for 14 glutamines (normal form) or a tract $(CAG)_2CAAAAGCAGCAA(CAG)_{77}$ coding for 83 glutamines

(expanded form) (Goto *et al.,* 1997) (hereafter referred as variant 1-1 and 1-1E, respectively),and (ii) MJD2-1 variant carrying a tract $(CAG)_2CAAAAGCAGCAA(CAG)_{22}$ coding for 28 glutamines (normal form) or a tract $(CAG)_2CAAAAGCAGCAA(CAG)_{78}$ coding for 84 glutamines (expanded form) (Chai *et al.,* 1997) (hereafter referred as variant 2-1 and 2-1E, respectively). The proteins were fused with the Green fluorescence protein (GFP), to allow subsequent observation of the ataxin-3 subcellular localization and of the formation of focal accumulation.

Yeast models of neurodegenerative diseases, like Parkinson and Huntington (reviewed in Braun *et al*., 2009) have been developed based on the hererologous expression of the disease-related proteins under the action of the Galactose inducible promoter, however this is a glucose-repressible system and changing the carbon source to galactose promotes pleiotropic effects on cellular metabolism leading to drastic genetic alterations. Therefore, these models have been questioned and alternative systems have been suggested such as the Tet On system (Garí *et al.,* 1997).

The Tet On system is an expression vector that does not require changes in carbon sources and does not cause any known effect in the cell metabolism. The Tet On system leads to the specific gene expression independent of the metabolic status of the cells. This system only requires the addition of tetracycline antibiotic or an analog (Bellí *et al*., 1998) to promote the gene expression not affecting the cellular metabolism of yeast cells (Garí *et al* 1997). In this sense, to construct the MJD models we have decided to use the ATXN3 genes under the control of the Tet On system leading to the specific gene expression independent of the metabolic status of the cells.

The details on the development of the different cloning strategies will be described below.

1.1 ATXN3 variants cloning

Plasmids construction is a crucial strategy in modern genetic manipulation. As of now, the common method for constructing plasmids is to digest specific DNA sequences with restriction enzymes and ligate the resulting DNA fragments with DNA ligase. In this

sense, to study ataxin-3 dynamics in living cells, we created an ATXN3-GFP fusion. For that, ATXN3 genes were first inserted in the pUG35 plasmid to allow the GFP fusion. To minimize the interference with the natural protein dynamics, the GFP was cloned in the C-terminal region, since the majority of proteins have in the N-terminal region targeting sequences responsible for their intracellular trafficking. Subsequently, ATXN3-GFP fusions were cloned in the final vector, the pCM252 (Euroscarf), that harbors the Tet On system, characterized by the presence of a transactivator, seven copies of TetO boxes and the CMV promoter.

1.1.1 Constructions of ATXN3 variants on pUG35 plasmid

The DNA fragments of ATXN3 genes of variant 1-1 (Figure 1) and 1-1E were amplified from pCMV plasmid (Silva-Fernandes *et al.,* 2010) and the ATXN3 genes of the variant 2-1 (Figure 2) and 2-1E were amplified from pEGFP-C_1 plasmid (Ferro *et al.,* 2007), using the specific primers 1, 2 and 3 (Table I), at specific PCR cycling conditions (Table II). The primers were designed to introduce restrictive enzyme cutting sites. As described in chapter 1, the ataxin-3 contains a Josephin protease domain, two or three ubiquitin interacting motifs (UIMs) (if is the variant 2-1 or the variant 1-1, respectively), and the polyglutamine domain, followed by a C-terminal stretch of hydrophobic aminoacids. Furthermore, in the variant 1-1 the 3' regions of the exon 10 are absent and the exon 11 is employed as 3' terminal sequence. Therefore, due to these differences, the forward primer for all the variants is similar, and it was designed using the *Bam*HI restrictive enzyme sequence and the reverse primers are different for each variant whereas the final sequence of the gene variants are different (Table I, primer 1). The reverse primers were designed with the final sequence of each variant and with the *Hind*III restrictive enzyme sequence (Table I, primers 2 and 3).

Figure 3, shows the results for the ATXN3 gene amplifications. The resultant fragments have a weight of 1086bp and 1293b to 1-1 and 1-1E forms, respectively, and 1095bp and 1269bp to 2-1 and 2-1E forms, respectively, corresponding to the molecular

weight of each ATXN3 gene and the sequences of restrictive enzymes, *Bam*HI and *Hind*III. The fragments have similar molecular weight, however as demonstrated in figure 3, it was possible to make the correlation between the observed band and the respective gene, using 1Kb ladder. This ladder allows high-quality molecular weight differentiation between 1000bp and 3000bp.

>ATXN3 variant 1 sequence

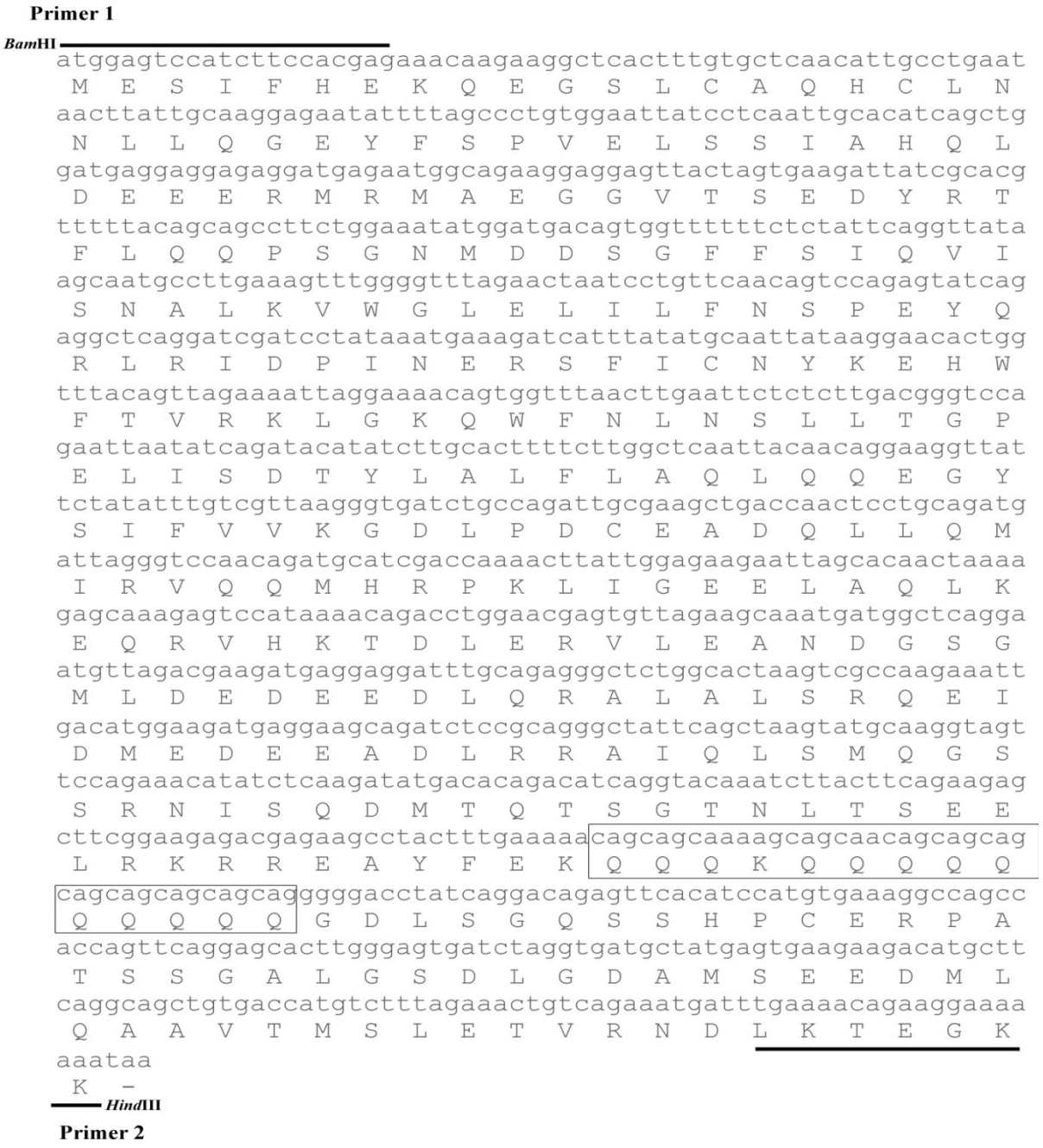

Figure 1. Nucleotide and protein sequences of ATXN3 variant 1 (obtained using OFR Finder from NCBI). Black boxes represent the Poly-Q tract of ATXN3 variant 1 with 14 glutamines and lines represent the sequence used to construct the primers (Accession no. U64820)

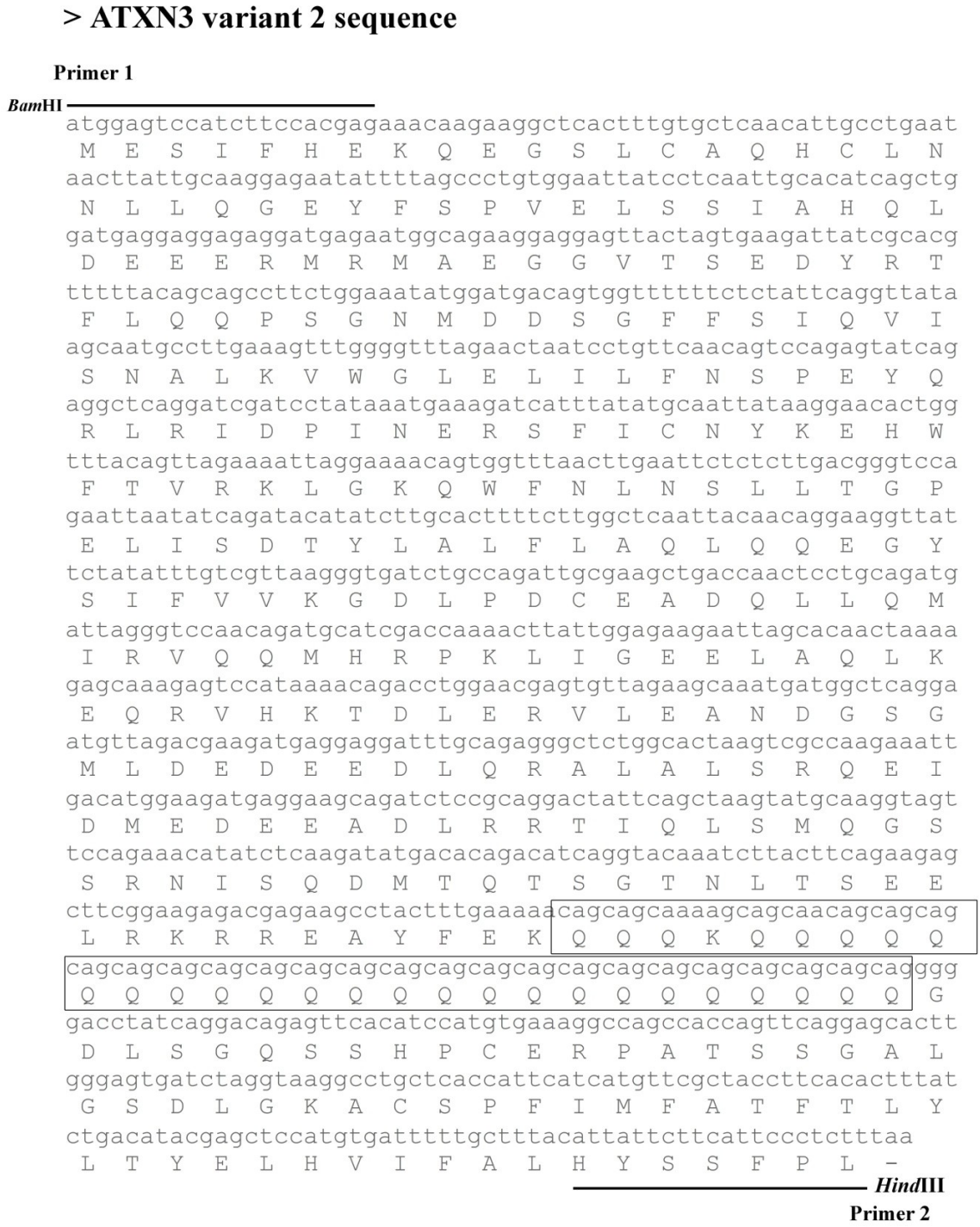

Figure 2. Nucleotide and protein sequences of ATXN3 variant 2 (obtained using OFR Finder from NCBI). Black boxes represent the Poly-Q tract of ATXN3 variant 2 with 28 glutamines and lines represent the sequence used to construct the primers (Accession no. U64821).

Table I. Primers used to amplify the ATXN3 variant genes.

Nº	Name	Sequence
1	MJDBamHI_F	5'-gcctggatccatggagtccatcttcc-3'
2	MJD1-1HindIII_R	5'-ccggaagctttttttttccttctgttttca-3'
3	MJD2-1HindIII_R	5´-ccggaagcttaagagggaatgaagaataat-3'
4	ApaIGFPpCM252_R	5'-ccgggcccttatttgtacaattc-3'

Table II. PCR cycling conditions performed to amplify the variants genes using primers 1, 2 and 3 (Table I).

Cycle step	Temperature	Time	Cycles
Initial Denaturation	94ºC	10 min	1
Denaturation	94ºC	45 seg	
Annealing	54ºC	30 seg	35
Extension	72ºC	2 min	
Final Extension	72ºC	10 min	1
	4ºC	hold	

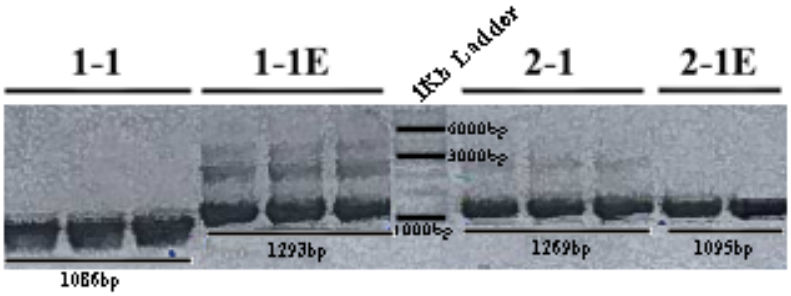

Figure 3. Amplification of ATXN3 variant genes. Variant 1 genes were amplified from pCMV plasmid (Silva-Fernandes *et al.,* 2010) and variant 2 genes were amplified from pEGFP-C_1 plasmid (Ferro *et al.,* 2007). The conditions for the performed amplifications were described on Table II and the primers used on Table I.

To introduce the inserts in the pUG35 plasmid, digestion of both pUG35 plasmid and the amplified fragments with the restriction enzymes *Bam*HI and *Hind*III was performed (Figure 4-A and 4-B). The restriction enzymes *Bam*HI and *Hind*III were selected given that they have only one restrictive site on plasmid and did not recognize any sequence to cut in the amplified sequences. Hence, the ligation of the amplified fragments to the linearized pUG35 with the T4 DNA Ligase (Fermentas) was carried out, followed by the *Escherichia coli* transformation with the resulted plasmids (Figure 4-C).

The obtained clones were analyzed and validated by the restriction enzymes assay. Thereby, relatively to the plasmids harboring the 1-1 and 2-1E variants, the restriction analysis was performed with *BamH*I and *Kpn*I restrictive enzymes, since the first one digest the plasmid in the local of the beginning of the gene, and the *Kpn*I enzyme digest after the GFP gene. Therefore, with this approach a confirmation of the gene insertion could be assessed. As expected, for the tested clones, a fragment around 5100bp, corresponding to pUG35 plasmid without the inserted gene and the intrinsic GFP, and a fragment with 2100bp corresponding to the inserts, ATXN3 genes fused with GFP gene were obtained. To confirm these results *Kpn*I restrictive enzyme was also used. As expected a single band with 7300bp, corresponding to the linearized plasmid with the genes, was obtained (Figure 5). The plasmids harboring the 1-1E and 2-1 variants were cut with *Eco*RI and *Eco*RV restrictive enzymes producing a single band with 7299bp and 7497bp, respectively (Figure 6). The restrictive treatment with *Eco*RI restrictive enzyme would linearized the pUG35 plasmid with the inserts since this enzyme have only one restriction site in the plasmid and no restriction site in the insert. As expected, only one band was obtained from *Eco*RI restrictive treatment, which corresponds to the linearized plasmid (Figure 6-A). It was also used *Eco*RV restrictive enzyme to confirm the results from *Eco*RI treatment. On pUG35 plasmid, this restrictive enzyme has two restrictive sites, nevertheless the variant genes insertion in the plasmid change the restrictive profile to a single restrictive local (Figure 6). In the strategy of plasmid construction confirmation, it was used two different set of restriction enzymes, since by this way it was possible to confirm the correct plasmid construction by two different approaches for each variant. Hence, the restrictive analyses with different restriction enzymes reveal the expected

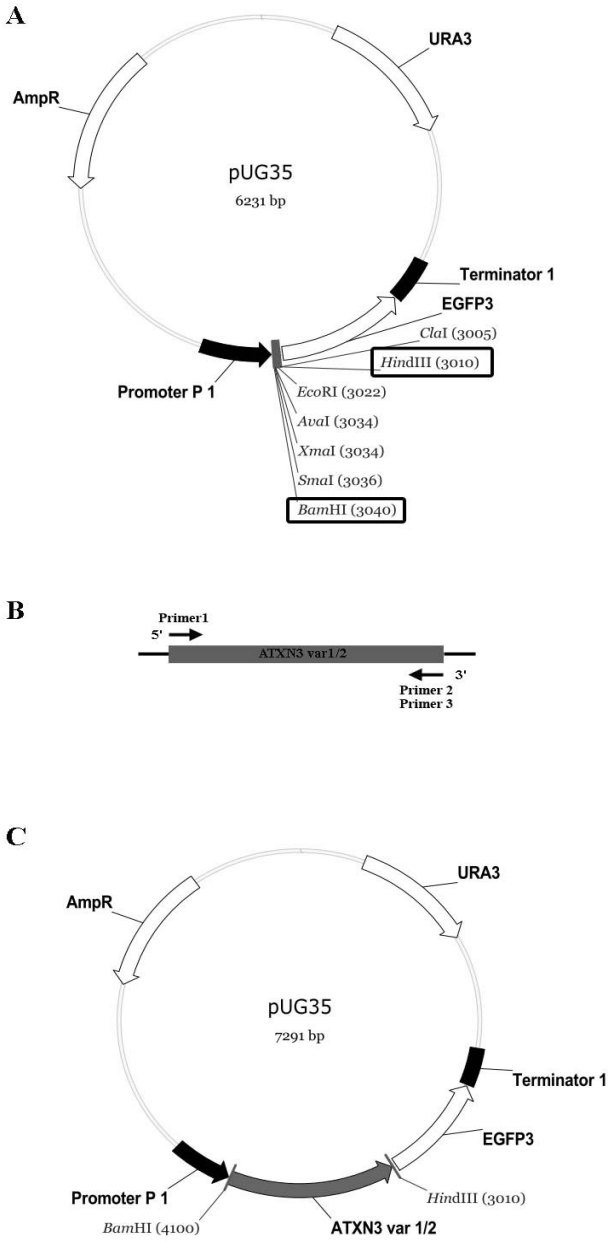

Figure 4. Schematic representation of molecular strategy to construct pUG35 plasmid harboring ATXN3 variant 1 and 2 genes (ATXN3 var1/2). A) Schematic representation of pUG35 plasmid, black boxes represents the restrictive enzymes used to digest the plasmid and to perform the ligation with gene fragments. B) Schematic representation of amplification of ATXN3 var1/2 genes. Primer 1 is the forward primer used to amplify the two variants. Primer 2 is the reverse primer for variant 1 genes and primer 3 the reverse primer for variant 2 genes. C) Schematic representation of pUG35 plasmid harboring the ATXN3 var1/2 genes. (The plasmids representation were performed using VectorNTI program).

results, indicating that apparently the four genes, 1-1, 1-1E, 2-1 and 2-1E, are correctly inserted in pUG35 plasmid.

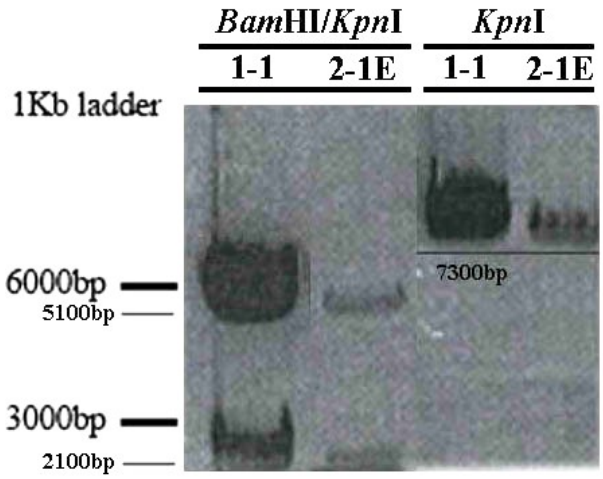

Figure 5. Restrictive endonuclease treatments to confirm the pUG35 harboring AXN3 genes constructions. Representative clone for variants 1-1 and 2-E tested by restrictive endonuclease treatment. To restrictive endonuclease treatments the restrictive enzymes *Bam*HI and *Kpn*I were used.

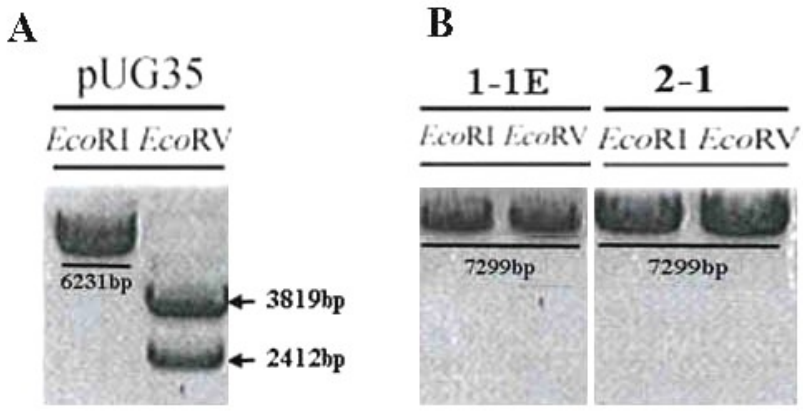

Figure 6. Restrictive endonuclease treatments to confirm the pUG35 harboring ATXN3 genes constructions. A) Restrictive endonuclease treatment of plasmid pUG35 using *Eco*RI and *Eco*RV restrictive enzymes. B) Representative clones for 1-1E and 2-1 genes inserted using *Eco*RI and *Eco*RV restrictive enzymes.

1.1.2 Construction of ATXN3-GFP fusion on pCM252 plasmid

To construct the final vector, the ATXN3-GFP genes were inserted in the plasmid harboring the Tet On system, the pCM252 (Figure 7-A and 7-B). The DNA fragments of the ATXN3-GFP variants were amplified from the pUG35 plasmids described in previous section. The specific PCR products were generated using the primers 1 and 4 (Table I), under specific PCR cycling conditions (Table III). Primer 1 (Table I), the forward primer, is equal for all the genes and was designed using the *Bam*HI restriction enzyme, to introduce the cut site for this enzyme. The reverse primer is composed by the final sequence of the GFP gene and the sequence of the *Apa*I restriction enzyme (Table I, primer 4). The presence of the correct ATXN3-GFP genes fragments was confirmed by the detection of 1803bp, 2010bp, 1812bp and 1990bp to 1-1 and 1-1E, 2-1 and 2-1E variants, respectively (Figure 8). The final vector was then constructed by digesting the plasmid pCM252 and the amplified fragments with *Bam*HI/*Apa*I that have only one restrictive site on plasmid and did not recognize any sequence to cut in the amplified sequences. The obtained PCR products were used to perform the ligation to the linear plasmid with the T4 DNA Ligase (Fermentas) and introduced in *E. coli* (Figure 8-C). Selection was performed on LB ampicillin plates. In order to identify positive clones, a restriction analysis of the plasmid DNA was performed using the restriction enzymes *Bam*HI and *Apa*I, which provided a digestive pattern with 2 fragments (Figure 9 and Table IV), one with the weight of the empty vector (7282bp) and the other with the weight of each amplified fragment (ATXN3-GFP genes). Thereby, the constructed vector harbors the variant genes designed as 1-1 and 1-1E, 2-1 or 2-1E in the plasmid polylinker, specifically at the *Bam*HI and *Apa*I sites. The vectors contain the reverse tTA transactivator gene, as well as the variant genes under the control of a $tetO_7$ promoter.

Table III. Program performed to amplify the variants genes fused to GFP gene using primers 1, 4 (Table I).

Cycle step	Temperature	Time	Cycles
Initial Denaturation	94ºC	10 min	1
Denaturation	94ºC	45 seg	
Annealing	54ºC	30 seg	30
Extension	68ºC	2 min	
Final Extension	68ºC	10 min	1
	4ºC	hold	

Table IV. Molecular weight of the fragments obtained from restrictive endonuclease treatment with *Bam*HI/*ApaI* for ATXN3-GFP fusion on pCM252 plasmid construction.

Plasmids constructed	BamHI/ApaI fragments size	Plasmid pCM252 fragments size
pCM252::1-1	1849bp	7282bp
pCM252::1-1E	2057bp	
pCM252::2-1	1859bp	
pCM252::2-1E	2049bp	

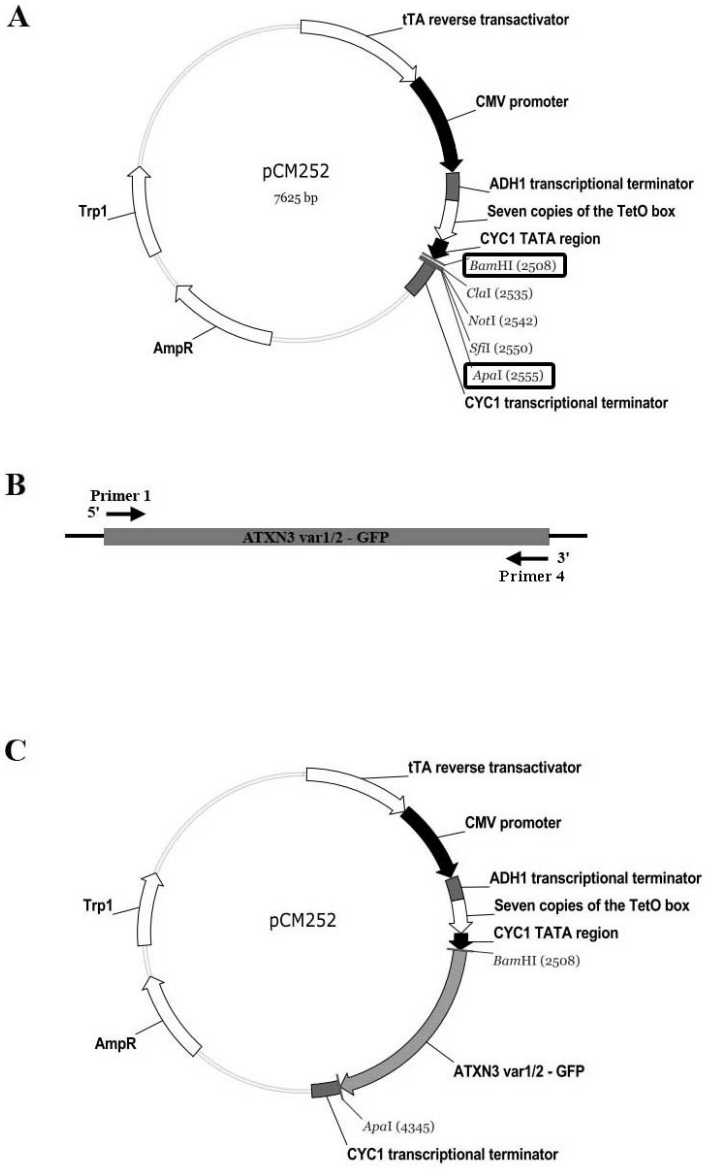

Figure 7. Schematic representation of molecular strategy to construct pCM252 plasmid harboring ATXN3 variant 1 and 2 genes fused with *GFP* gene (ATXN3 var1/2 + GFP). A) Schematic representation of pCM252 plasmid, black boxes represents the restrictive enzymes used to digest the plasmid, to perform the ligation with gene fragments. B) Schematic representation of amplification of ATXN3 var1/2 genes fused with *GFP* gene. Primer 1 is the forward primer used to amplify the two variants. Primer 4 is the reverse primer constructed with *GFP* sequence to all the variants. C) Schematic representation of pCM252 plasmid harboring the ATXN3 var1/2 genes fused with *GFP* gene (The plasmids representations were performed using VectorNTI program).

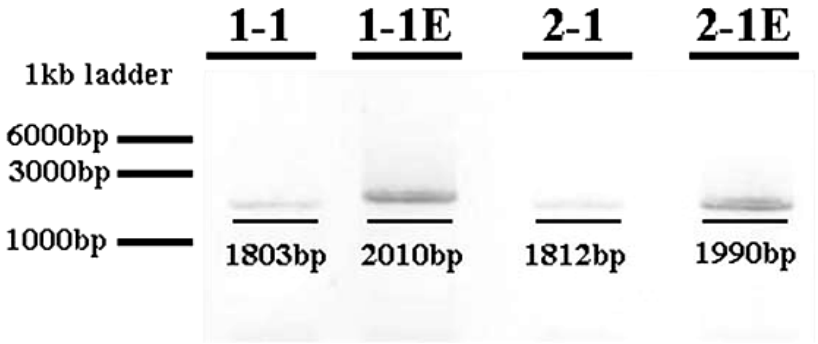

Figure 8. Amplification of ATXN3 variant genes fused with *GFP* gene. The genes were amplified from pUG35 plasmid construction. The PCR cycling conditions for the performed amplifications were described on Table III and the primers used on Table I.

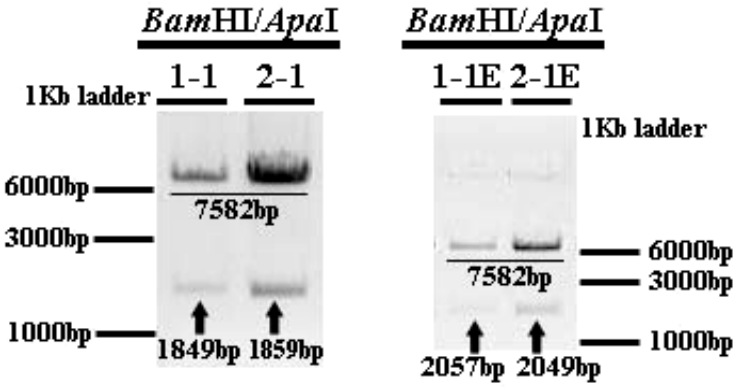

Figure 9. Restrictive endonuclease treatments to confirm the pCM252 harboring ATXN3 genes insertions. Clones for each gene construction were tested. To restrictive endonuclease treatment was used *Bam*HI and *Apa*I restrictive enzymes. Black arrows represent the clones selected as positives to send to sequencing.

1.2 ATXN3-GFP genes sequencing

To validate the constructed plasmids, DNA from pCM252:: ATXN3-GFP genes was isolated using the ZR plasmid Miniprep (Zymo Research) and confirmed by sequencing (Eurofins MWG Operon, Ebersberg, Germany) using primers 1 and 4, described in table I.

As expected, sequencing results showed that the plasmid pCM252::1-1 harbored a polyQ tract with 13 CAGs, while the expanded form of the variant 1, the plasmid pCM252::1-1E, had 92 CAGs (Figure 10). However, relatively to the variant 2, unlike what was expected, normal and expanded forms presented similar number of CAGs repeats, 13 and 16, respectively (data not shown). The unexpected results could occur due to the elevated number of CAGs repeats since it is described that loops of repeat-containing DNA can cause either expansions or contractions during amplifications, when the scanning occurs in the template (Møllersen *et al*., 2010). Consequently, relatively to the variant 2, new assays must be executed to select clones with a polyQ tract around 80 CAGs repeats. For that, new PCR conditions, as well as new Taq DNA polymerases with proofreading activity will be tested to avoid unexpected results.

A

Alignment for pCM252::1-1

```
                    ....|....| ....|....| ....|....| ....|....|
                       5         15         25         35
pCM252::1-1         ATGGAGTCCA TCTTCCACGA GAAACAAGAA GGCTCACTTT
pCM252::1-1 seq     ATGGAGTCCA TCTTCCACGA GAAACAAGAA GGCTCACTTT

                    ....|....| ....|....| ....|....| ....|....|
                       45         55         65         75
pCM252::1-1         GTGCTCAACA TTGCCTGAAT AACTTATTGC AAGGAGAATA
pCM252::1-1 seq     GTGCTCAACA TTGCCTGAAT AACTTATTGC AAGGAGAATA

                    ....|....| ....|....| ....|....| ....|....|
                       85         95         105        115
pCM252::1-1         TTTTAGCCCT GTGGAATTAT CCTCAATTGC ACATCAGCTG
pCM252::1-1 seq     TTTTAGCCCT GTGGAATTAT CCTCAATTGC ACATCAGCTG

                    ....|....| ....|....| ....|....| ....|....|
                       125        135        145        155
pCM252::1-1         GATGAGGAGG AGAGGATGAG AATGGCAGAA GGAGGAGTTA
pCM252::1-1 seq     GATGAGGAGG AGAGGATGAG AATGGCAGAA GGAGGAGTTA

                    ....|....| ....|....| ....|....| ....|....|
                       165        175        185        195
pCM252::1-1         CTAGTGAAGA TTATCGCACG TTTTTACAGC AGCCTTCTGG
pCM252::1-1 seq     CTAGTGAAGA TTATCGCACG TTTTTACAGC AGCCTTCTGG

                    ....|....| ....|....| ....|....| ....|....|
                       205        215        225        235
pCM252::1-1         AAATATGGAT GACAGTGGTT TTTTCTCTAT TCAGGTTATA
pCM252::1-1 seq     AAATATGGAT GACAGTGGTT TTTTCTCTAT TCAGGTTATA

                    ....|....| ....|....| ....|....| ....|....|
                       245        255        265        275
pCM252::1-1         AGCAATGCCT TGAAAGTTTG GGGTTTAGAA CTAATCCTGT
pCM252::1-1 seq     AGCAATGCCT TGAAAGTTTG GGGTTTAGAA CTAATCCTGT

                    ....|....| ....|....| ....|....| ....|....|
                       285        295        305        315
pCM252::1-1         TCAACAGTCC AGAGTATCAG AGGCTCAGGA TCGATCCTAT
pCM252::1-1 seq     TCAACAGTCC AGAGTATCAG AGGCTCAGGA TCGATCCTAT

                    ....|....| ....|....| ....|....| ....|....|
                       325        335        345        355
pCM252::1-1         AAATGAAAGA TCATTTATAT GCAATTATAA GGAACACTGG
pCM252::1-1 seq     AAATGAAAGA TCATTTATAT GCAATTATAA GGAACACTGG

                    ....|....| ....|....| ....|....| ....|....|
                       365        375        385        395
pCM252::1-1         TTTACAGTTA GAAAATTAGG AAAACAGTGG TTTAACTTGA
pCM252::1-1 seq     TTTACAGTTA GAAAATTAGG AAAACAGTGG TTTAACTTGA

                    ....|....| ....|....| ....|....| ....|....|
                       405        415        425        435
pCM252::1-1         ATTCTCTCTT GACGGGTCCA GAATTAATAT CAGATACATA
pCM252::1-1 seq     ATTCTCTCTT GACGGGTCCA GAATTAATAT CAGATACATA

                    ....|....| ....|....| ....|....| ....|....|
                       445        455        465        475
pCM252::1-1         TCTTGCACTT TTCTTGGCTC AATTACAACA GGAAGGTTAT
pCM252::1-1 seq     TCTTGCACTT TTCTTGGCTC AATTACAACA GGAAGGTTAT

                    ....|....| ....|....| ....|....| ....|....|
                       485        495        505        515
pCM252::1-1         TCTATATTTG TCGTTAAGGG TGATCTGCCA GATTGCGAAG
pCM252::1-1 seq     TCTATATTTG TCGTTAAGGG TGATCTGCCA GATTGCGAAG

                    ....|....| ....|....| ....|....| ....|....|
                       525        535        545        555
pCM252::1-1         CTGACCAACT CCTGCAGATG ATTAGGGTCC AACAGATGCA
pCM252::1-1 seq     CTGACCAACT CCTGCAGATG ATTAGGGTCC AACAGATGCA

                    ....|....| ....|....| ....|....| ....|....|
                       565        575        585        595
pCM252::1-1         TCGACCAAAA CTTATTGGAG AAGAATTAGC ACAACTAAAA
pCM252::1-1 seq     TCGACCAAAA CTTATTGGAG AAGAATTAGC ACAACTAAAA

                    ....|....| ....|....| ....|....| ....|....|
                       605        615        625        635
pCM252::1-1         GAGCAAAGAG TCCATAAAAC AGACCTGGAA CGAGTGTTAG
pCM252::1-1 seq     GAGCAAAGAG TCCATAAAAC AGACCTGGAA CGAGTGTTAG

                    ....|....| ....|....| ....|....| ....|....|
                       645        655        665        675
pCM252::1-1         AAGCAAATGA TGGCTCAGGA ATGTTAGACG AAGATGAGGA
pCM252::1-1 seq     AAGCAAATGA TGGCTCAGGA ATGTTAGACG AAGATGAGGA

                    ....|....| ....|....| ....|....| ....|....|
                       685        695        705        715
pCM252::1-1         GGATTTGCAG AGGGCTCTGG CACTAAGTCG CCAAGAAATT
pCM252::1-1 seq     GGATTTGCAG AGGGCTCTGG CACTAAGTCG CCAAGAAATT

                    ....|....| ....|....| ....|....| ....|....|
                       725        735        745        755
pCM252::1-1         GACATGGAAG ATGAGGAAGC AGATCTCCGC AGGGCTATTC
pCM252::1-1 seq     GACATGGAAG ATGAGGAAGC AGATCTCCGC AGGGCTATTC

                    ....|....| ....|....| ....|....| ....|....|
                       765        775        785        795
pCM252::1-1         AGCTAAGTAT GCAAGGTAGT TCCAGAAACA TATCTCAAGA
pCM252::1-1 seq     AGCTAAGTAT GCAAGGTAGT TCCAGAAACA TATCTCAAGA

                    ....|....| ....|....| ....|....| ....|....|
                       805        815        825        835
pCM252::1-1         TATGACACAG ACATCAGGTA CAAATCTTAC TTCAGAAGAG
pCM252::1-1 seq     TATGACACAG ACATCAGGTA CAAATCTTAC TTCAGAAGAG
```

B

Alignment for pCM252::1-1E

```
                    ....|....| ....|....| ....|....| ....|....|
                       5         15         25         35
pCM252::1-1E        ATGGAGTCCA TCTTCCACGA GAAACAAGAA GGCTCACTTT
pCM252::1-1E seq    ATGGAGTCCA TCTTCCACGA GAAACAAGAA GGCTCACTTT

                    ....|....| ....|....| ....|....| ....|....|
                       45         55         65         75
pCM252::1-1E        GTGCTCAACA TTGCCTGAAT AACTTATTGC AAGGAGAATA
pCM252::1-1E seq    GTGCTCAACA TTGCCTGAAT AACTTATTGC AAGGAGAATA

                    ....|....| ....|....| ....|....| ....|....|
                       85         95         105        115
pCM252::1-1E        TTTTAGCCCT GTGGAATTAT CCTCAATTGC ACATCAGCTG
pCM252::1-1E seq    TTTTAGCCCT GTGGAATTAT CCTCAATTGC ACATCAGCTG

                    ....|....| ....|....| ....|....| ....|....|
                       125        135        145        155
pCM252::1-1E        GATGAGGAGG AGAGGATGAG AATGGCAGAA GGAGGAGTTA
pCM252::1-1E seq    GATGAGGAGG AGAGGATGAG AATGGCAGAA GGAGGAGTTA

                    ....|....| ....|....| ....|....| ....|....|
                       165        175        185        195
pCM252::1-1E        CTAGTGAAGA TTATCGCACG TTTTTACAGC AGCCTTCTGG
pCM252::1-1E seq    CTAGTGAAGA TTATCGCACG TTTTTACAGC AGCCTTCTGG

                    ....|....| ....|....| ....|....| ....|....|
                       205        215        225        235
pCM252::1-1E        AAATATGGAT GACAGTGGTT TTTTCTCTAT TCAGGTTATA
pCM252::1-1E seq    AAATATGGAT GACAGTGGTT TTTTCTCTAT TCAGGTTATA

                    ....|....| ....|....| ....|....| ....|....|
                       245        255        265        275
pCM252::1-1E        AGCAATGCCT TGAAAGTTTG GGGTTTAGAA CTAATCCTGT
pCM252::1-1E seq    AGCAATGCCT TGAAAGTTTG GGGTTTAGAA CTAATCCTGT

                    ....|....| ....|....| ....|....| ....|....|
                       285        295        305        315
pCM252::1-1E        TCAACAGTCC AGAGTATCAG AGGCTCAGGA TCGATCCTAT
pCM252::1-1E seq    TCAACAGTCC AGAGTATCAG AGGCTCAGGA TCGATCCTAT

                    ....|....| ....|....| ....|....| ....|....|
                       325        335        345        355
pCM252::1-1E        AAATGAAAGA TCATTTATAT GCAATTATAA GGAACACTGG
pCM252::1-1E seq    AAATGAAAGA TCATTTATAT GCAATTATAA GGAACACTGG

                    ....|....| ....|....| ....|....| ....|....|
                       365        375        385        395
pCM252::1-1E        TTTACAGTTA GAAAATTAGG AAAACAGTGG TTTAACTTGA
pCM252::1-1E seq    TTTACAGTTA GAAAATTAGG AAAACAGTGG TTTAACTTGA

                    ....|....| ....|....| ....|....| ....|....|
                       405        415        425        435
pCM252::1-1E        ATTCTCTCTT GACGGGTCCA GAATTAATAT CAGATACATA
pCM252::1-1E seq    ATTCTCTCTT GACGGGTCCA GAATTAATAT CAGATACATA
```

```
                    ....|....| ....|....| ....|....| ...|....|
                       845        855        865        875
pCM252::1-1         CTTCGGAAGA GACGAGAAGC CTACTTTGAA AAACAGCAGC
pCM252::1-1 seq     CTTCGGAAGA GACGAGAAGC CTACTTTGAA AAACAGCAGC

                    ....|....| ....|....| ....|....| ....|....|
                       885        895        905        915
pCM252::1-1         AAAAGCAGCA ACAGCAGCAG CAGCAGCAGC AGCAGGGGGA
pCM252::1-1 seq     AAAAGCAGCA ACAGCAGCAG CAGCAGCAGC AGCAGGGGGA

                    ....|....|
                       925
pCM252::1-1         CCTATCAGGA
pCM252::1-1 seq     CCTATCAGGA
```

Figure 10. Results from variant 1 genes sequencing. A) Alignment result using 1-1 original sequence (pCM252::1-1) (described in Figure 2) compared with the results from sequencing (pCM252::1-1 seq). B) Alignment result using 1-1E original sequence (pCM252::1-1) (described in Figure 3) compared with the results from sequencing (pCM252::1-1 seq).

2. Yeast model for Huntington's disease

Huntington's disease (HD), like Machado-Joseph's Disease (MJD), is another polyQ disorder, characterized by the presence of a polyQ tract on huntingtin protein. A major hallmark of HD is the presence of brain lesion composed of inclusions that contain the protein huntingtin (reviewed in Barral *et al.,* 2004 and Borrel-Pagès *et al.,* 2006). The length of the polyQ tract in huntingtin is directly correlated with kinetics of its aggregation in vitro and with severity of the disease in HD patients, and indirectly with the disease onset (Duyao *et al.,* 1993).

The huntingtin protein has no homologous protein in yeast cells, thus the yeast model for HD was developed to allow the heterologous expression of huntingtin in yeast, as described for MJD (previous section). Most of the studies use a yeast model of HD based on the huntingtin expression under the action of a galactose-inducible promoter, requiring a carbon source exchange to promote huntingtin expression (Solans *et al*., 2006 and Hughes *et al*., 2001). Once more, taking into account that, carbon source changes can promote pleiotropic effects on cellular metabolism, a yeast model of HD based on the expression of the HTT gene modulated by a tetracycline-regulated vector (Tet On system) was used. This yeast model of HD was kindly provided by Dr. Fulvio Reggiori (University Medical Centre, Utrecht, The Netherlands) and employs the W303-1a strain (Euroscarf) harboring a plasmid containing the first exon of HTT gene, with a polyQ tract of 25 glutamines (25Q) and 103 glutamines (103Q), under the action of the Tet On system. HTT genes are fused with GFP gene on the C-terminal region to assess the subcellular localization of huntingtin proteins. In accordance with the observations in HD patients and other models (Cowan *et al.*, 2003; Landles *et al*., 2010 and Rockabrand *et al*., 2007), the toxicity of huntingtin in yeast cells also depends on the length of polyQ tract, being that the expression of HTT gene with 103Q is more toxic than the expression of HTT with 25Q. In fact, in yeast models of HD in which the huntingtin gene is under the action of a galactose-inducible promoter, the expression of the huntingtin fragment with the polyQ length in the pathogenic range (103Q) produced cellular toxicity, while expression of the same construct containing the non-expanded polyQ tract (25Q) presented no damaging effects (reviewed in Outeiro and Giorgini, 2006). Furthermore, expression of the HTT gene with 103Q was

shown to lead to the formation of more protein aggregates compared with cells expressing the HTT gene with 25Q (Krobitsch and Lindquist, 1999).

HD is the most studied polyQ disorder and although the findings obtained in the study of this disease are not easily and directly extrapolated to other polyQ disorders, it is crucial to understand the basic molecular mechanisms shared by all the polyQ disorders and the ones that are specific for a particular one (Ross *et al.,* 1999).

One of the most prominent questions regarding the pathogenesis of neurodegenerative diseases such as HD is the role of autophagy. Autophagy has emerged as a key player in neurodegenerative diseases, nonetheless, its role remains controversial, given that an autophagic induction could promote the clearance of misfolded proteins, however, with time, an excessive autophagy induction can occur, leading to neurodegeneration and cell death (reviewed in Cuervo *et al.,* 2005 and Rajawat and Bossis, 2010). In this sense, it is relevant to evaluate if during aging the stimulation of autophagy, due to persistent levels and/or a dysregulation regarding its activity and even to its selectivity, may compromise the cell viability.

The yeast models of HD employing a Tet On System are well characterized in our laboratory. The toxicity promoted by the heterologous expression of HTT was accompanied along the yeast lifespan after induction in the different phase of yeast cell growth: exponential, diauxic and stationary, 4, 24 hours and 4 days (corresponding to 2 days of chronological life span (CLS)), respectively (represented in Figure 11).

The data shows that the expression of huntingtin 103Q form has a greater toxic effect when compared to normal huntingtin 25Q form, in accordance with the descriptions in other models (reviewed in Truant, 2003) (Figure 12-B and 12-C). The pronounced toxicity of huntingtin 103Q form compared to the 25Q is independent of the cell growth phase where the expression was induced and thus independent of the cell physiologic state, as demonstrated by the survival data, in which, independently of the growth phase, between 10 and 12 days of aging, cells expressing huntingtin 103Q form exhibited about 50% survival compared with almost 100% of cells harboring the huntingtin 25Q form or the empty vector (Figure 12). Although the expression of huntingtin 103Q form did not result in significant alterations in the CLS with cell survival until around day 22, it is possible to

observe that its expression in aged cells results in a decrease of survival in a short period of time (Figure 12-C).

The expression of the toxic protein, huntingtin 103Q, could induce the foci formation. Examination of cells, using epifluorescent microscopy analysis in the studied conditions, allowed the visualization of GFP fused with the huntingtin forms. Independently of the growth phase, the cells expressing the huntingtin 103Q form reveal the presence of several small *foci* in the cytoplasm, being more pronounced after 48h of expression induction (Figures 14, 16 and 18, untreated panels), in accordance with already described (Duennwald *et al.,* 2006a; Duennwald *et al.,* 2006b; Rockabrand *et al.*, 2007 and Atwal *et al.*, 2007). Additionally, the cells expressing the normal huntingtin 25Q form displayed GFP dispersed in the cytoplasm in all the studied conditions.

Therefore, these results showed that the expression of the huntingtin 103Q form during yeast life cycle enhanced toxicity (Figure 12), accompanied with *foci* formation (Figures 14; 16 and 18, untreated panels). Furthermore, this first characterization allowed the possibility of perform posterior studies related, specifically, to the modulation of the autophagic process in cells expressing the huntingtin with a poly-Q stretch of 25 or 103 CAGs, as described in the next section.

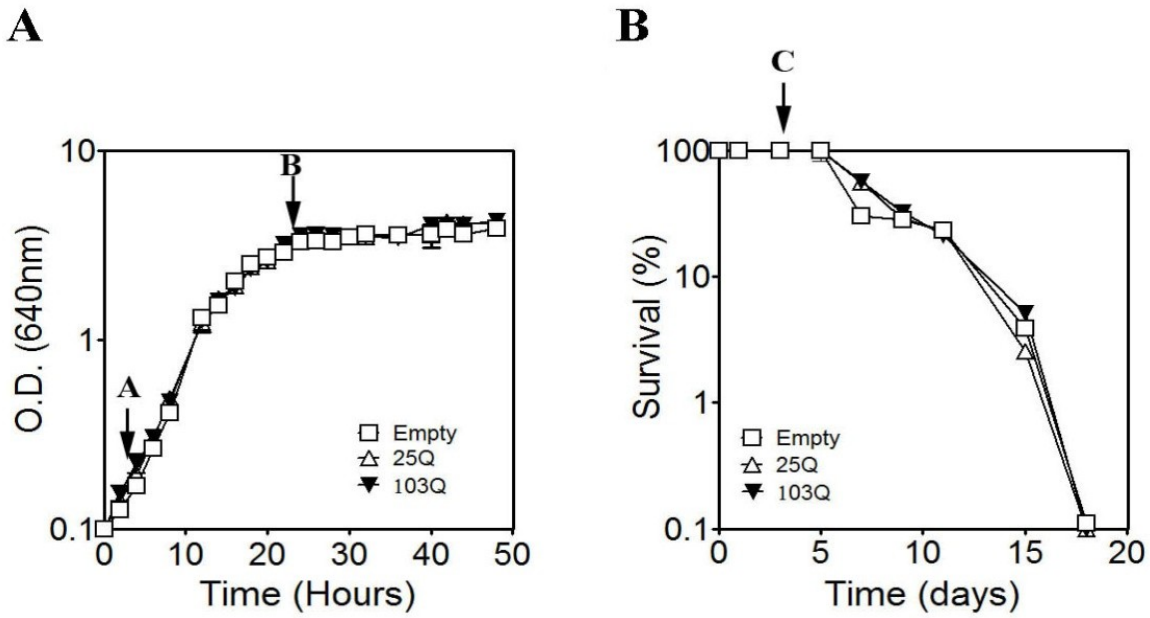

Figure 11. Characterization of the life cycle of yeast model for Huntington's disease harboring the Tet On system. The study of yeast growth and lifespan was performed without the protein expression for strains harboring the HTT gene with 25 glutamines (25Q) or 103 glutamines (103Q) as well as the empty vector. A, represents cell survival assessed by densitometry until stationary phase (48h) and B, represents cell survival assessed by CFUs counts during chronological life span. Arrows represents the different time points to promote the induction of expression of the disease-related proteins. A- 4 hours; B- 24 hours and C- 4 days*.

* These results were obtained by Maria de Belém Marques in scope of her PhD thesis.

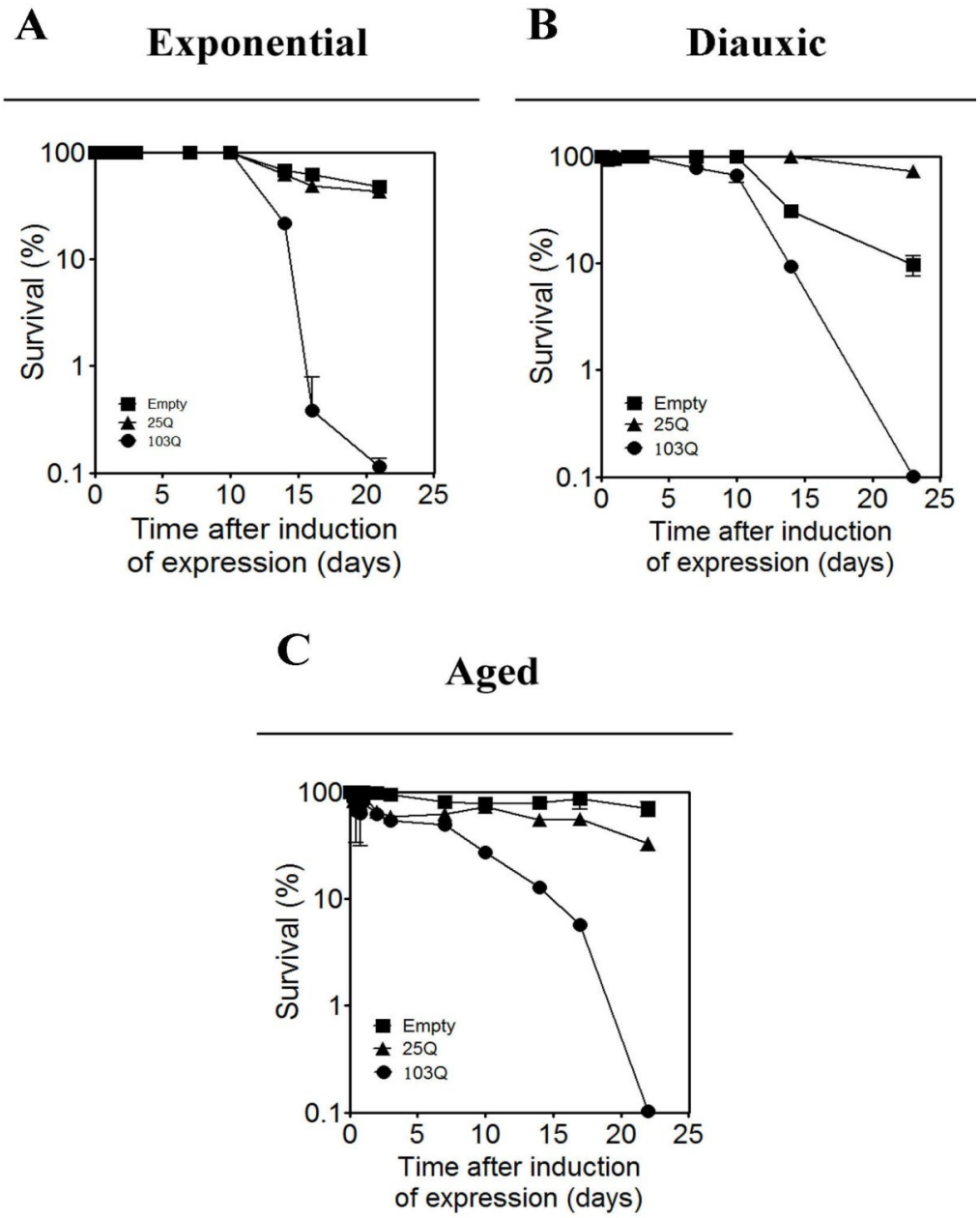

Figure 12. Chronological life span of cells expressing the Huntington disease-related proteins, under the control of the Tet On system, at different growth phases. Survival determined by CFU´s (Colony forming units) of yeast cells whereas the expression of the huntingtin with 25 glutamines (25Q), 103 glutamines (103Q) or harboring the respective empty vector was induced at the exponential (A), diauxic (B) or stationary (aged) (C) phases*.

* These results were obtained by Maria de Belém Marques in scope of her PhD thesis.

2.1 The role of autophagy in Huntington's yeast model

In recent year, the autophagic process has been implicated in several human diseases, including in Huntington's disease (HD). Autophagy has been implicated in the degradation of aggregated-prone proteins associated with neurodegenerative disorders (reviewed in Mizushima *et al.,* 2008). Nevertheless, the role of autophagy in the pathogenesis of neurodegenerative diseases remains controversial. Furthermore, autophagy has been implicated in several different biological functions such as aging, an inevitable physiological process characterized by a progressive accumulation of damaged macromolecules and organelles associated with the decline in housekeeping mechanisms (reviewed in Cuervo *et al*., 2005).

To study the relevance of autophagy during different phases of yeast life span, the huntingtin expression was induced, again, at exponential, diauxic and stationary (corresponding to 2 days of CLS) phases, 4, 24 hours and 4 days, respectively as described before. To facilitate the study of the involvement of autophagy, it is possible to develop different strategies to modulate the autophagic pathway in yeast cells, such as the usage of mutant strains in specific *ATG* genes (Autophagy related genes) or the pharmacologic manipulation of central players of the autophagic pathway. In this work it was decided to pharmacologically inhibit the autophagic pathway using chloroquine, an effective autophagic inhibitor nontoxic that does not impair cellular energy metabolism, protein synthesis or viability, specifically it is an inhibitor of vacuolar acidification, which, in turn, is required for the fusion of autophagosomes with vacuoles (reviewed in Maiuri *et al.,* 2007). Therefore, at the same time that we promoted the huntingtin expression, autophagy was inhibited, by the addition of chloroquine to the culture medium.

2.1.1 HTT expression in exponential growth phase cells: the effect of the inhibition of autophagy

Autophagy inhibition, due to the addition of chloroquine, in exponential cells expressing the huntingtin 25Q form or harboring the empty vector induced a decreased in CLS (Figure 13-A and 13-B), contrarily to what was observed without chloroquine treatment. Surprisingly, autophagic inhibition allowed an increased on the CLS of exponential cells expressing the toxic huntingtin form, 103Q (Figure 13-C). These data indicate that in a physiologic context, autophagy is a crucial process to cell, probably removing unwanted intracellular components and to provide energy (reviewed in Cuervo, 2008), since autophagic inhibition in cells harboring the empty vector or expressing the non-toxic huntingtin form demonstrated a drastic reduction in the CLS (only 20 days). Furthermore, in the pathologic context of huntingtin 103Q expression, the autophagy apparently has a deleterious role, because under autophagy inhibition these cells exhibited a CLS of around 28 days (Figure 13-C), contrasting with the 22 days observed without the chloroquine treatment, originating a CLS increased of about 30%.

When we proceeded with microscopic analysis, we observed that exponential cells expressing the huntingtin expanded polyQ tract (103Q), under chloroquine treatment exhibited the presence of *foci*, as expected; however, the cells presented a decreased number of the *foci*, when compared with what was observed without chloroquine treatment (Figure 14). Furthermore, the majority of the cells, due to the presence of chloroquine, presented a large *foci*, that could correspond to aggresomes, which are formed by convergence of smaller inclusions at the centrosomes via microtubule-based transport (Büttner *et al.,* 2010) and due to the impairment or overwhelmed of the cellular degradation machinery. Additionally, the aggresomes formation apparently acts as cytoprotective mechanism.

Consistently with survival data, exponential cells expressing the huntingtin 25Q form revealed a fluorescence pattern similar to one observed without autophagy inhibition, uncovered by the visualization of GFP dispersed in the cytoplasm. At exponential phase induction, the autophagic inhibition, due to the chloroquine treatment, stimulated a protective effect to cells expressing the toxic huntingtin 103Q form. Contrarily, a negative

effect, due to autophagy inhibition, is exhibited by cells expressing the normal huntingtin 25Q form.

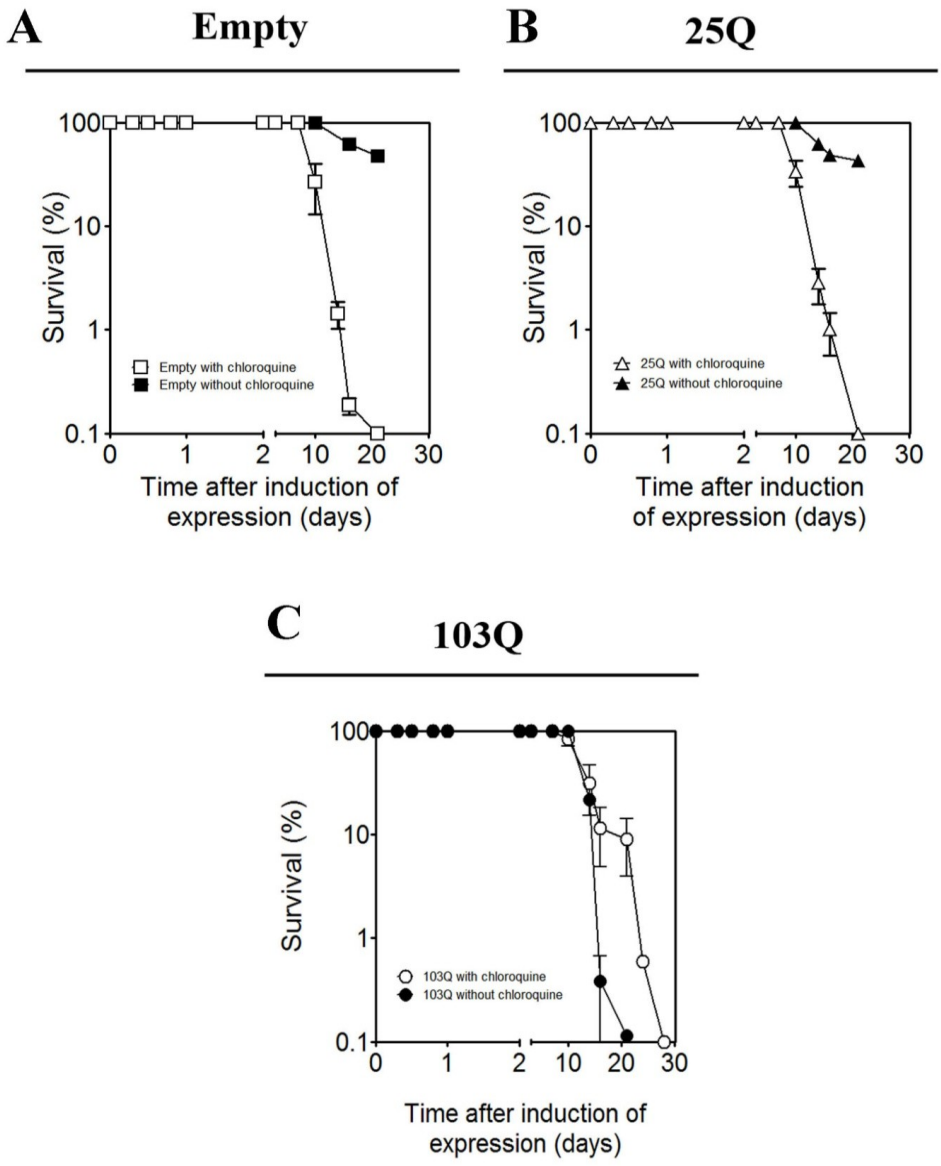

Figure 13. Chronological life span of cells expressing the Huntington disease-related proteins, induced at exponential phase, with or without chloroquine treatment. Survival determined by CFU´s of yeast cells whereas the expression of the huntingtin with 25 glutamines (25Q) (A), 103 glutamines (103Q) (B) or harboring the respective empty vector (B) was induced at the exponential phase, with or without chloroquine treatment.

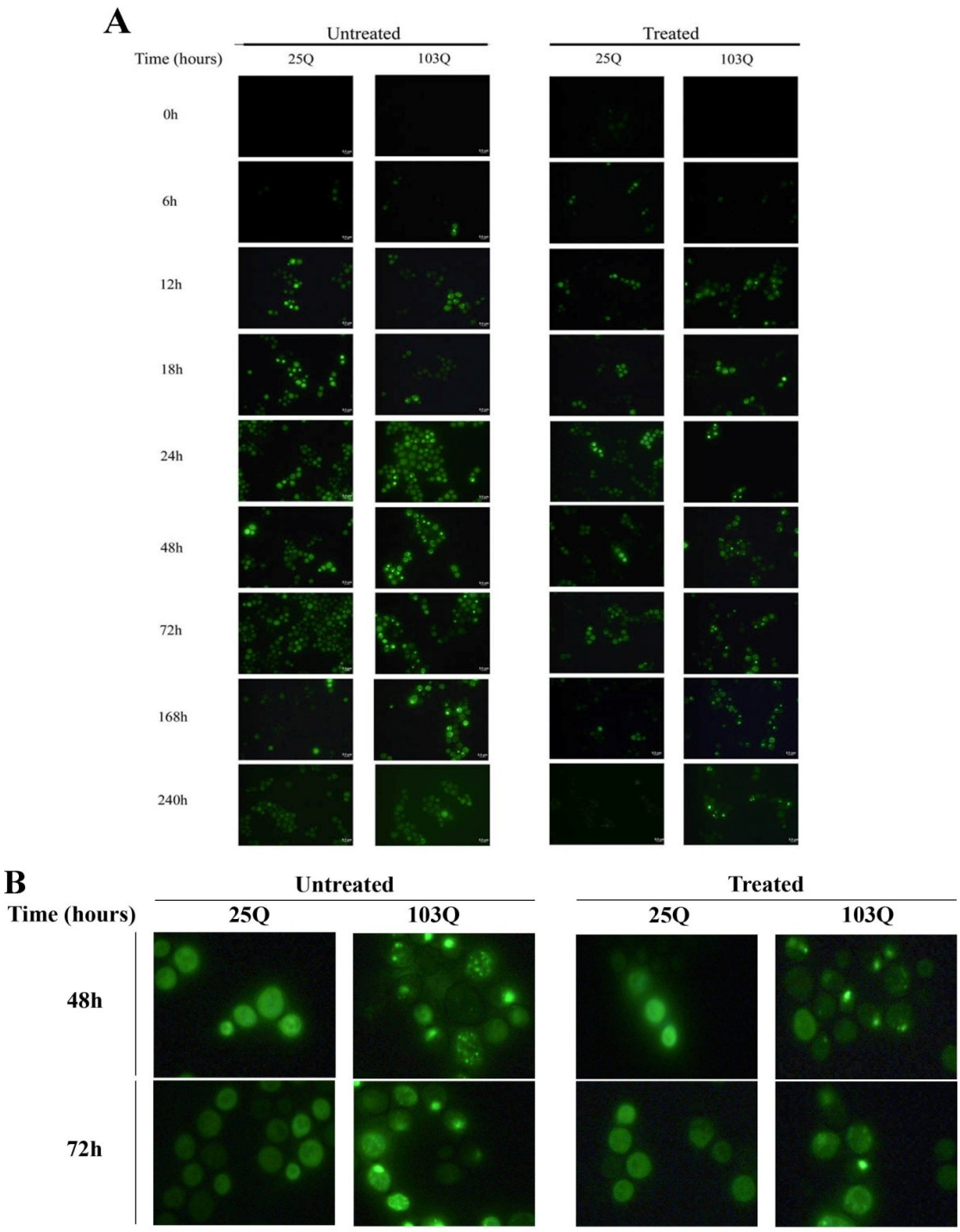

Figure 14. Epifluorescent microscopy analysis of GFP pattern of exponential cells expressing the Huntington disease-related proteins, with or without chloroquine treatment. A) Fluorescence microscopy analysis of yeast cells expressing the huntingtin 25Q or 103Q forms, induced at the exponential phase, with or without chloroquine treatment. B) Epifluorescence photographs details of yeast cells expressing the huntingtin 25Q or 103Q forms, with or without chloroquine treatment, at 48h and 72h.

2.1.2 HTT expression in diauxic growth phase cells: the effect of the inhibition of autophagy

The diauxic phase is characterized by a decreased growth rate and by a switching metabolism from glycolysis to respiration (Galdieri *et al.,* 2010), that consequently promotes the acquisition of intrinsic stress resistance.

The presence of chloroquine that inhibits autophagy, in diauxic cells expressing the toxic huntingtin form, 103Q, induce a moderated extension in CLS (Figure 15-C), in contrast to the observations made in cells without chloroquine treatment. Diauxic cells expressing the huntingtin 25Q form or harboring the empty vector exhibit no alterations in the CLS (Figure 15-A and 15-B). Knowing the higher resistance of diauxic cells, the data seems to indicate that during diauxic phase, the cells acquire a higher capacity to deal with stress inducers, since the diauxic cells expressing the huntingtin 25Q form or harboring the empty vector presented similar CLS independently of the chloroquine presence. Furthermore, in diauxic cells expressing the huntingtin 103Q form, although the chloroquine treatment (autophagy inhibition) allowed the reduction of the deleterious effects observed in cells without chloroquine treatment, it only was observed a moderated extension in the CLS (Figure 15-C), probably due to higher resistance capacity of these cells.

Consistently with described in section 2.1.1, cells expressing the toxic huntingtin 103Q form showed the presence of *foci* (Figure 16), however, due to the presence of chloroquine, the *foci* were in a reduced number. Additionally, there are innumerous cells that present a single large *foci*, probably representing an aggresome. Diauxic cells expressing the huntingtin 25Q form displayed GFP disperse to the cytoplasm, similar to observed without chloroquine treatment (Figure 16) and consistent with survival data.

At diauxic phase induction, the autophagy inhibition induces a moderate protector effect to cells expressing the huntingtin 103Q form. Nevertheless, at this phase, the cells expressing the normal huntingtin 25Q form have the capacity to adapt to the medium alterations, having a response independently of the chloroquine treatment.

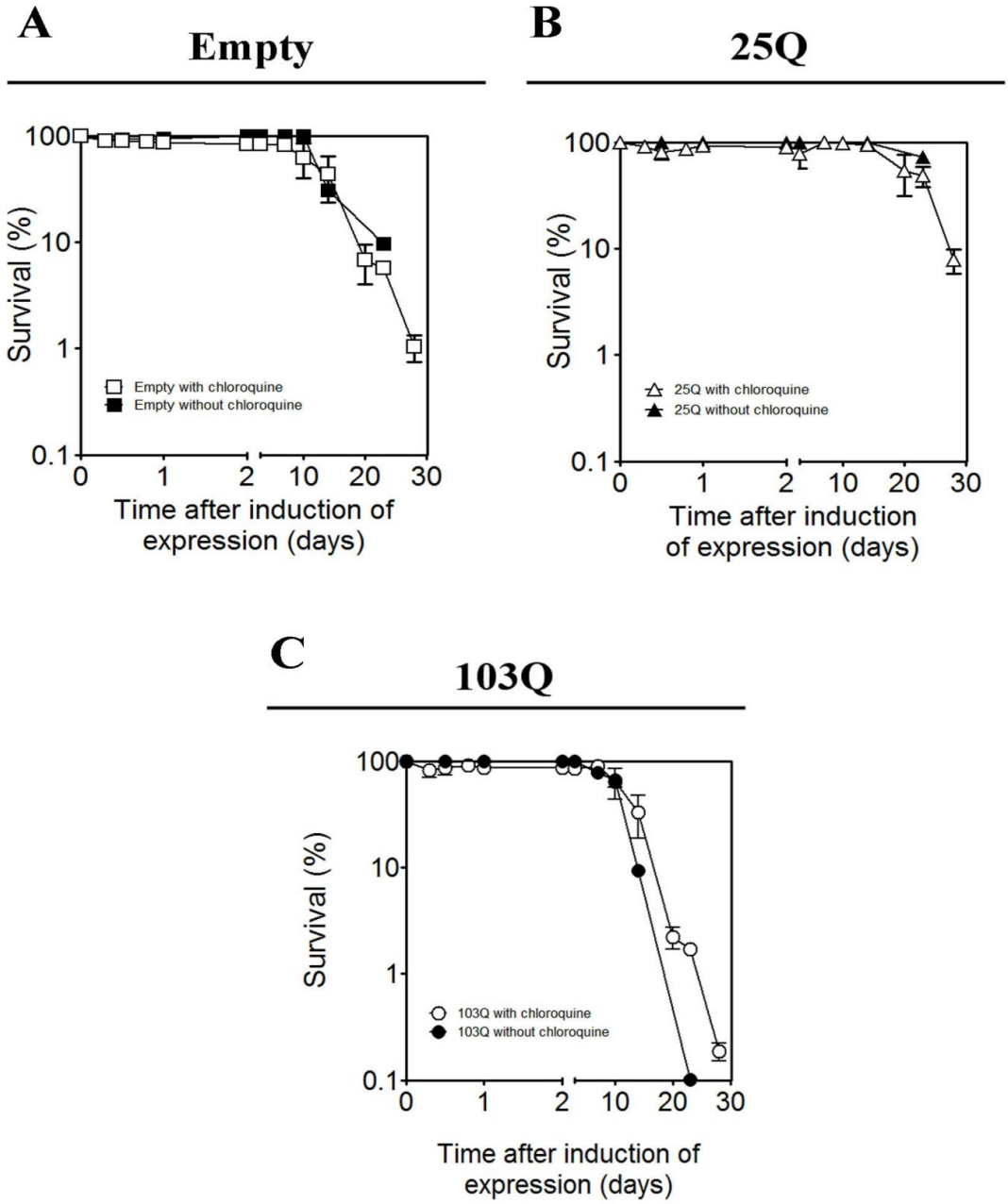

Figure 15. Chronological life span of cells expressing the Huntington disease-related proteins, induced at diauxic phase, with or without chloroquine treatment. Survival determined by CFU´s of yeast cells whereas the expression of the huntingtin with 25 glutamines (25Q) (A), 103 glutamines (103Q) (B) or harboring the respective empty vector (B) was induced at the diauxic phase, with or without chloroquine treatment.

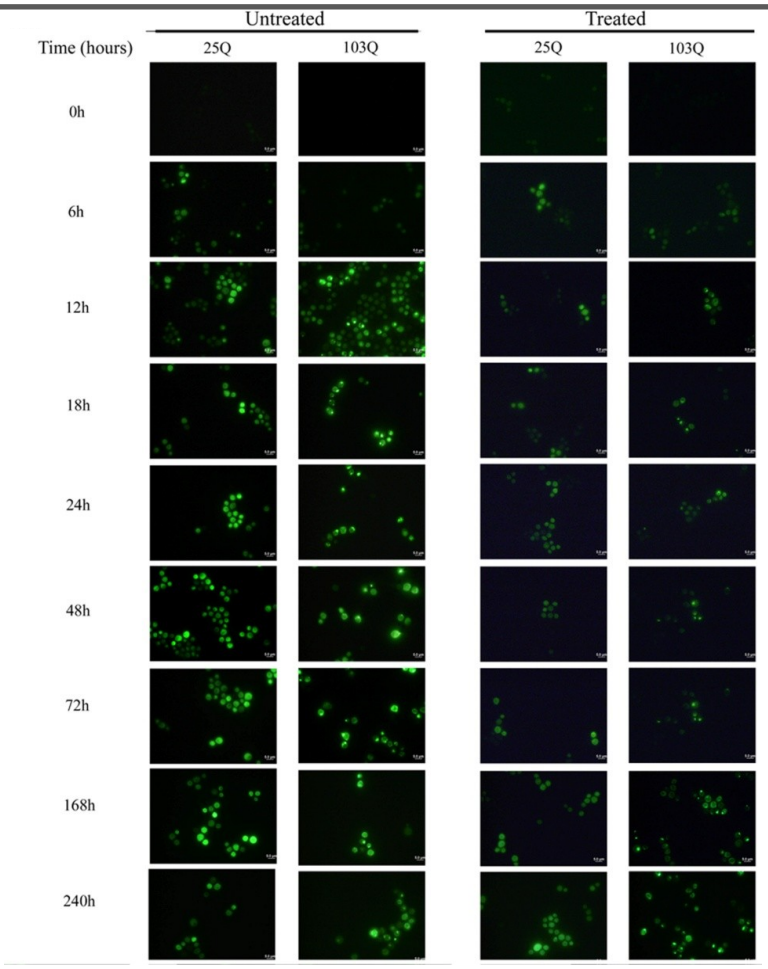

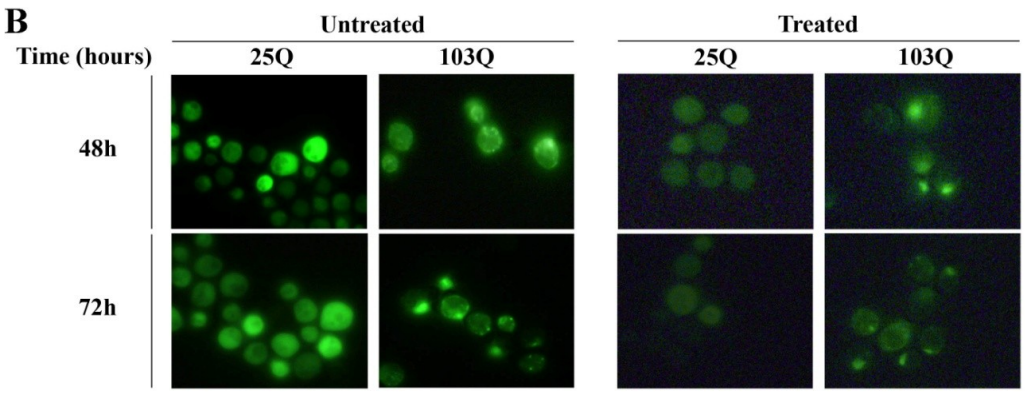

Figure 16. Epifluorescent microscopy analysis of GFP pattern of diauxic cells expressing the Huntington disease-related proteins, with or without chloroquine treatment. A) Fluorescence microscopy analysis of yeast cells expressing the huntingtin 25Q or 103Q forms, induced at the diauxic phase, with or without chloroquine treatment. B) Epifluorescence photographs details of yeast cells expressing the huntingtin 25Q or 103Q forms, with or without chloroquine treatment, at 48h and 72h.

2.1.3 HTT expression in aged cells: the effect of the inhibition of autophagy

The autophagy inhibition, in stationary cells expressing the huntingtin 103Q form, leads to a CLS extension, comparatively to what was observed without chloroquine treatment (Figure 17-C). In contrast, the autophagic inhibition induced toxicity in cells harboring the empty vector (Figure 17-A), disclosed by a decrease in CLS, while had no significant effects in the CLS of cells expressing the normal huntingtin 25Q form (Figure 17-B).

During stationary growth phase under huntingtin 103Q expression, the cells manifest an autophagy induction, potentiated, on one hand by physiological factors, like the starvation for carbon and nitrogen sources, which inactivate the TOR pathway (reviewed in Høyer-Hansen and Jäättelã, 2007). On other hand, most probably, the expression of the huntingtin 103Q forms induces, by themselves, autophagy. Therefore, apparently, excessive autophagy activation occurs and might have nefast effects for cell survival. Thus, the inhibition of autophagy leads to a CLS extension of about 30% to cells expressing the huntingtin 103Q form (Figure 17-B).

Under physiologic conditions, at stationary phase, autophagy has a prominent role, on the clearance of the unwanted intracellular contents and especially in the supply of essential cell energy. In this sense, when the autophagy is inhibited in cells harboring the empty vector, we observed a drastic CLS reduction (Figure 17-A). Contrarily, in cells expressing the normal huntingtin 25Q form, a balance between the anti and pro-death autophagy roles is occurring, and the cell is able to adapt to situation of autophagy inhibition resulting in the maintenance of cell survival. Hence, the CLS of cells was similar, independently of the chloroquine presence.

Autophagic inhibition has protective effects as observed in cells expressing the huntingtin toxic form was also confirmed by the reduction in the number of *foci* present in the cellular cytoplasm. Furthermore, the majority of cells presented large *foci*, which could correspond to the aggresome, as described above, which apparently as a cytoprotective effect. As expected, in cells expressing the normal huntingtin 25Q form, the GFP were detected dispersed in the cytoplasm (Figure 18).

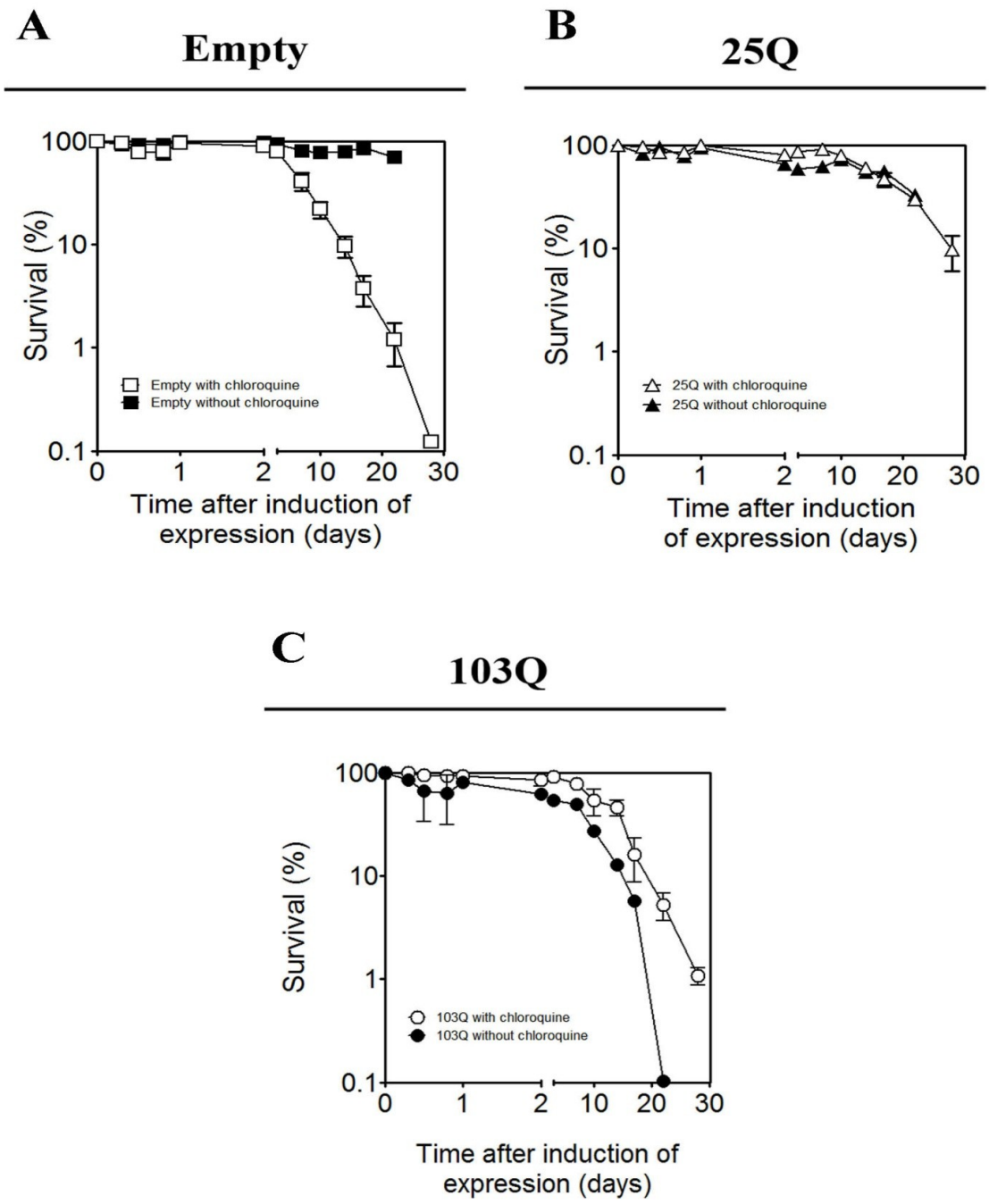

Figure 17. **Chronological life span of cells expressing the Huntington disease-related proteins, induced at stationary (aged) phase, with or without chloroquine treatment.** Survival determined by CFU´s of yeast cells whereas the expression of the huntingtin with 25 glutamines (25Q) (A), 103 glutamines (103Q) (B) or harboring the respective empty vector (B) was induced at the stationary phase, with or without chloroquine treatment.

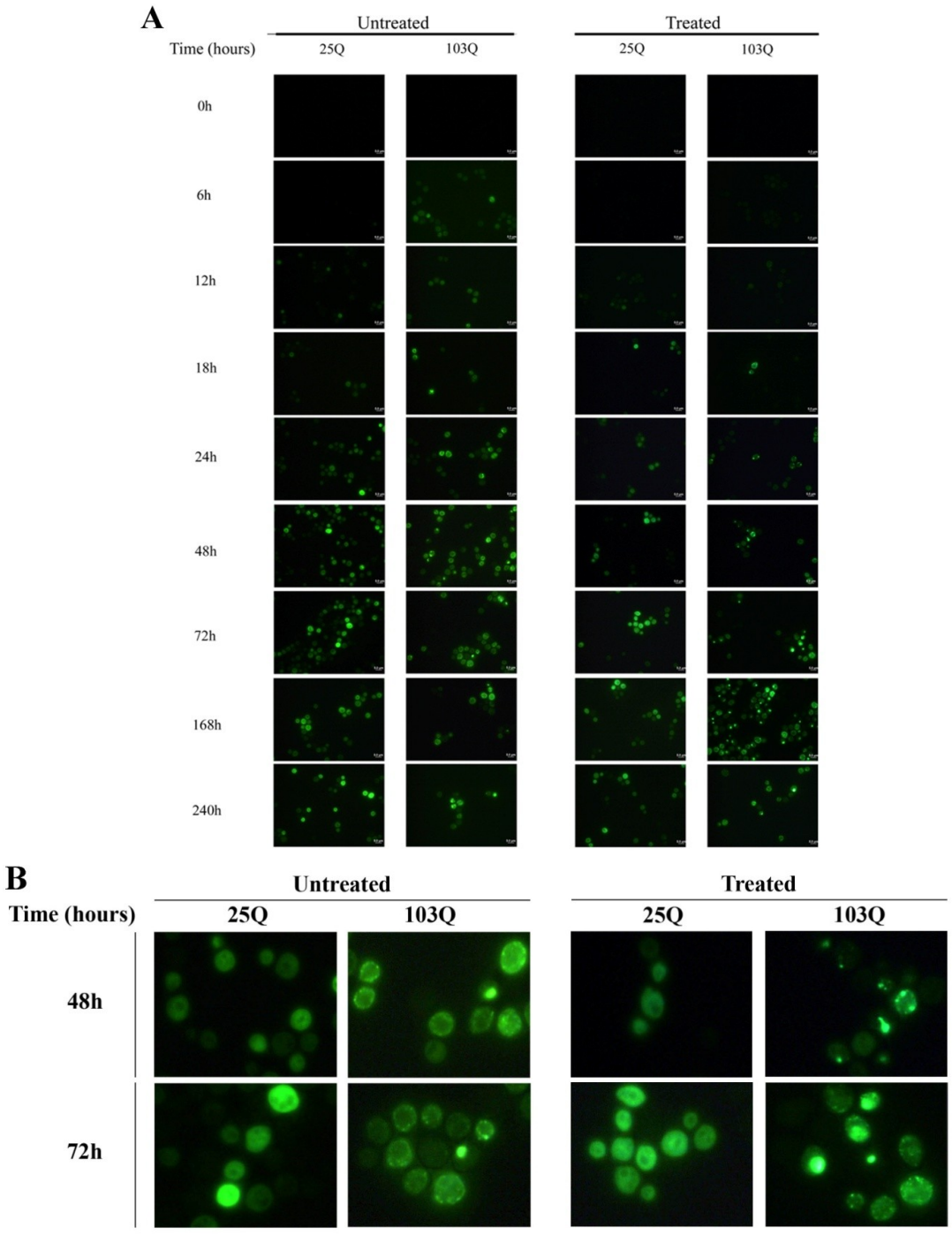

Figure 18. Epifluorescent microscopy analysis of GFP pattern of aged cells expressing the Huntington disease-related proteins, with or without chloroquine treatment. A) Fluorescence microscopy analysis of yeast cells expressing the huntingtin 25Q or 103Q forms, induced at the stationary (aged) phase, with or without chloroquine treatment. B) Epifluorescence photographs details of yeast cells expressing the huntingtin 25Q or 103Q forms, with or without chloroquine treatment, at 48h and 72h.

Autophagy inhibition, carried out by chloroquine treatment, resulted in protection to cells expressing the toxic huntingtin 103Q form. This protection was observed independently of the physiologic state, at which protein expression was promoted (Table V), being less pronounced at the diauxic phase. These data apparently indicate that under the pathologic context of huntingtin expression, the autophagic process plays a deleterious role. Furthermore, the obtained results with the microscopic analysis corroborate the CLS analysis, since, the chloroquine treatment induced a decrease of the *foci* formation, and more specifically, in innumerous cells the presence of an unique large *foci*, that could correspond to aggresomes, which apparently is formed in order to overcome cellular damage, was observed. The cells harboring the empty vector or expressing the huntingtin 25Q form exhibit different response to the autophagy inhibition, according to the phase at which is forced the protein expression, as represented in Table V. Therefore, cells at which the protein expression was induced at the diauxic phase apparently have a higher capacity to deal with the autophagy inhibition.

These data demonstrate that the autophagic process has a role in the disease pathogenesis has an inducer of cell death in functional and aged cells.

Table V. Chonological life span (CLS) analysis of cells harboring the empty vector or expressing the huntingtin 25Q or 103Q forms at different growth phases: exponential, diauxic or stationary. The symbols represent the alterations observed in the CLS under chloroquine treatment comparatively to the CLS obtained without treatment to each studied condition.

	Empty Vector	25Q	103Q
Exponential	-	-	+
Diauxic	NA	NA	+
Stationary (aged)	-	NA	+

+ increase; - decrease; NA no alterations

IV. Discussion

IV. Discussion

Protein folding is a cellular process that acts in new synthesized proteins to promote their correct three-dimensional structure. Nevertheless some mutations or transcriptional errors, RNA splicing and translation errors can lead to protein misfolding. These misfolding proteins can by degraded by cellular machinery or leads to formation of protein aggregates (Gao and Hu, 2008). The accumulation of misfolded proteins gives rise to dysfunction of living systems. There are a number of serious diseases which have as a common aspect the inappropriate folding of a particular protein. Polyglutamine (polyQ) diseases, such Machado-Joseph's (MJD) and Huntington's diseases (HD), is a group of neurodegenerative diseases caused by the accumulation of misfolding diseases, being characterized by the presence of a CAG tract in related gene that causes a polyglutamine tract in the related protein (The Huntington's Disease Collaborative Research Group, 1993 and Kawaguchi *et al.,* 1994) this polyglutamine tract does not let get the correct folding of related proteins. The PolyQ diseases are a very heterogeneous group of human disorders being HD the most studied one. In the last decades it has been speculated that some of the characteristic hallmarks of HD disease could be easily extrapolated to other PolyQ diseases (Ross *et al.,* 1999). Nevertheless, there are important specificities that must be taken into consideration. In this sense, with this work, we aimed to develop a yeast model for MJD. The study of neurodegenerative diseases using yeast models has been done through the expression of the human related gene under the control of a galactose (GAL) inducible promoter (reviewed in Braun *et al*., 2009). Although GAL promoters allow a strong gene expression, which has the advantage of producing high concentrations of disease related protein and thus a strong phenotype, this promoter requires the changing of the carbon source from glucose, the yeast preferred one, to galactose. Changing the carbon source from glucose to galactose, besides inducing the heterologous gene expression, also promotes a strong genetic remodeling due the catabolic repression endorsed by glucose. Thus, to discard the effects of transferring cells to galactose we aimed to develop a yeast model in which the human genes are under the control of tetracycline. The final results of plasmid sequentiation show that the construction of pCM252::1-1 and pCM252::1-1E was successful.With these vectors, successfully constructed, is now necessary transform yeast cells to start the growth and toxicity characterization when the genes were expressed. After this characterization we had constructed the first model for MJD, which has never been

described before. Nonetheless, it is still required more work to construct the plasmids harboring the 2-1 variant genes, since the sequentiation analysis revealed that 2-1 and 2-1E genes lost part of the polyQ tract, presenting a polyQ tract with 14 and 16 CAGs, respectively. These are common phenomena when trying to amplify genes with a high number of CAGs repeats since the formation of loops of repeat-containing DNA can cause either expansions or contractions during amplification (Møllersen *et al*., 2010). In this line, in the future it is necessary to perform new assays, with variant 2, to select clones with a polyQ tract with 80 CAGs repeats, the pathogenic form. For this, new PCR conditions as well as new Taq DNA polymerases with proof reading activity will be used to avoid unexpected results. Nevertheless, this work allowed the development of vectors harboring the variant 1 genes, for ataxin-3 protein, being the most study variant in other models. In the near future, these vectors will allow the construction of first yeast model for Machado-Joseph's disease.

Huntington's disease is the most well study disease into polyQ disease group, having been developed several models, including the yeast model using the GAL promoter as well as the Tet On System to promote heterologous expression of disease related-proteins (Duennwald *et al.,* 2006a and Duennwald *et al.,* 2006b). Studies from different models for HD showed that the expression of huntingtin with a expanded polyQ tract leads to decreased cell survival and some propose that autophagic process can be involved in the cell rescue of cell death (Mizhushima *et al.,* 2008 and Pan *et al.,* 2008). Keeping in mind the new knowledge for the possible involvement of autophagic process in Huntington's disease, we aimed to address the effect of autophagic inhibition on cells expressing normal and pathogenic huntingtin. Additionally, and given that HD disease is a late onset disease, we aimed to understand if autophagic inhibition can produce different outcomes depending on age of the cells and their physiological state. As previously described, the results herein presented show that the expression of the pathogenic huntingtin (103Q) is highly toxic for yeast cells and that the toxicity seems to be independent on the cellular physiological growth phase. The toxicity of the pathogenic huntingtin (103Q) is associated to foci formation as has previously been described (Duennwald *et al.,* 2006a and Duennwald *et al.,* 2006b). Surprisingly when autophagy was inhibited, by chloroquine a nontoxic

inhibitor, the toxicity of the huntingtin (103Q) is reduced and cells present an extension of CLS independently of the yeast growth phase in which protein expression was induced but more pronounced in aged cells. In contrast, the inhibition of autophagy when cells are expressing the huntingtin 25Q form in exponential phase results in a decrease of CLS and has no effect in diauxic phase cells. The results obtained with cells in diauxic phase of growth are in accordance with the increased capacity of these cells to deal with stress inducers, due to the metabolic shift from fermentation to respiration, which encompasses several cellular changes (Galdieri *et al.*, 2010). Although requiring further studies, the data obtained provide new insights on the role of autophagy in HD pathogenesis. The results suggest that autophagy instead of having a protective effect on the clearance of protein aggregates could be detrimental for the pathogenesis of HD. Autophagy is a crucial cellular survival process in a physiologic context but aging might lead to a deregulation of this process increasing its activity or decreasing its selectivity. In aged cells expressing the pathogenic huntingtin demonstrate that inhibition of autophagy had a protective role, that is more pronounced compared with other physiological states, demonstrating that autophagy play a deleterious role in this situation, apparently caused by the impairment of cellular mechanisms due to the age physiological state of cells (reviewed in Cuervo *et al.*, 2005 and Rajawat and Bossis, 2010). Furthermore the formation of large aggregates, in cells expressing pathogenic huntingtin that could correspond to aggresomes, seems to act as cytoprotective mechanism in these cells when the autophagy is impaired.

Taken all the data obtained it was demonstrate that the progress of the disease was associated with aging and with autophagic process which is apparently impaired due to aging process. To be accepted the hypothesis that autophagy has a negative effect in aged cells expressing the pathogenic huntingtin more studies must be performed, such as the use of autophagy enhancers and inhibitors (such as genetically abrogation of *ATG* genes) as well as the analysis of the autophagy selectivity in aged cells.

V. References

V. References

Alberts, B, Jonhnson, A., Lewis, J., Raff, M., Roberts, K. and Walter, P. 2002. How Cells Read the Genome: From DNA to Protein. *Molecular Biology of The Cell.* (Garland Science eds), 4ª ed., pp 356-360, New York.

Albrecht, M., Golatta, M., Wüllner, U. and Lengauer, T. 2004. Structural and functional analysis of ataxin-2 and ataxin-3. Eur J Biochem. **271**(15): 3155-70.

Atwal, R. S., Xia, J., Pinchey, D., Taylor, J., M. Epand, Richard and Truant, Ray. 2007. Huntingtin has a membrane association signal that can modulate huntingtin aggregation, nuclear entry and toxicity. Hum Mol Genet. **16**(21): 2600-15.

Barral, J. M., Broadley, S. A., Schaffar, G. and Hartle, F. U. 2004. Roles of molecular chaperones in protein misfolding diseases. Semin. Cell Dev Biol. **15**(1): 17-29.

Bates, G. P. and Davies, S. W. 1997. Transgenic mouse models of neurodegenerative disease caused by CAG/polyglutamine expansions. Mol Med Today. **3**(11): 508-15.

Bellí, G., Garí, E., Piedrafita, L., Aldea, M. and Herrero, E. 1998. An activator/repressor dual system allows tight tetracycline-regulated gene expression in budding yeast. Nucleic Acids Res. **26**(4): 942-947.

Berke, S. J., Chai, Y., Marrs, G. L., Wen, H. and Paulson, H. L. 2005. Defining the role of ubiquitin-interacting motifs in the polyglutamine disease protein, ataxin-3. J Biol Chem. **280**(36): 32026-34.

Bettencourt, C., *et al.* 2009. Increased transcript diversity: novel splicing variants of Machado-Joseph disease gene (ATXN3). Neurogenetics. **11**(2): 193-202.

Borrell-Pagès, M., Zala, D., Humbert, S. and Saudou, F. 2006. Huntington's disease: from huntingtin function and dysfunction to therapeutic strategies. Cell Mol Life Sci. **63**(22): 2642-60.

Braun, R. J., Buttner, S., Ring, S. Kroemer, G. and Madeo, F. 2009. Nervous yeast: modeling neurotoxic cell death. Trends Biochem. Sci. **35**(3): 135-44.

Brignull, H. R., Morley, J. F., Garcia, S. M. and Morimoto, R. I. 2006. Modeling polyglutamine pathogenesis in C. elegans. Methods in Enzymology. **412**: 256-82.

Burnett, B., Li, F. and Pittman, R. N. 2003. The polyglutamine neurodegenerative protein ataxin-3 binds polyubiquitylated proteins and has ubiquitin protease activity. Hum Mol Genet. **12**(23): 3195-205.

Buttner, S. *et al*. 2010. Synphilin-1 enhances alpha-synuclein aggregation in yeast and contributes to cellular stress and cell death in a Sir2-dependent manner. PLoS One. **5**(10): e13700.

Cattaneo, E., Zuccato, C. and Tartari, M. 2005. Normal huntingtin function: an alternative approach to Huntington's disease. Nat Rev Neurosci. **6**(12): 919-30.

Chai, Y., Koppenhafer, S. L., Shoesmith, S. J., Perez, M. K. and Paulson, H. L. 1999. Evidence for proteasome involvement in polyglutamine disease: localization to nuclear inclusions in SCA3/MJD and suppression of polyglutamine aggregation in vitro. Hum Mol Genet. **8**(4): 673-82.

Chen, Q., Ding, Q. and Keller, J. N. 2005. The stationary phase model of aging in yeast for the study of oxidative stress and age-related neurodegeneration. Biogerontology. **6**(1): 1-13.

V. References

Chou, A., Yeh, T., Ouyang, P., Chen, Y., Chen, S. and Wang, H. 2008. Polyglutamine-expanded ataxin-3 causes cerebellar dysfunction of SCA3 transgenic mice by inducing transcriptional dysregulation. Neurobiol Dis. **31**(1): 89-101.

Cowan, K. J., Diamond, M. I. and Welch, E. J. 2003. Polyglutamine protein aggregation and toxicity are linked to the cellular stress response. Hum Mol Genet. **12**(12): 1377-91.

Cuervo, A. M. 2008. Autophagy and aging: keeping that old broom working. Trends Genet. **24**(12): 604-12.

Cuervo, A. M., Bergamini, E., Brunk, U. L., Dröge, W., Ffrench, M. and Terman, A. 2005. Autophagy and aging: the importance of maintaining "clean" cells. Autophagy. **1**(3): 131-40.

D'Abreu, A., França Jr., M. C., Paulson, H. L. and Lopes-Cendes, I. 2010. Caring for Machado-Joseph disease: current understanding and how to help patients. Parkinsonism Relat Disord. **16**(1): 2-7.

Ding, W., Ni, H., Gao, W., Yoshimori, T. Stolz, D. B., Ron, D. and Yin, X. 2007. Linking of autophagy to ubiquitin-proteasome system is important for the regulation of endoplasmic reticulum stress and cell viability. Am J Pathol. **171**(2): 513-24.

Doss-Pepe, E. W., Stenroos, E. S., Johnson, W. G. and Madura, K. 2003. Ataxin-3 interactions with rad23 and valosin-containing protein and its associations with ubiquitin chains and the proteasome are consistent with a role in ubiquitin-mediated proteolysis. Mol Cell Biol. **23**(18): 6469-83.

Duennwald, M. L., Jagadish, S., Giorgini, F., Muchowski, P. J. and Linquist, S. 2006a. A network of protein interactions determines polyglutamine toxicity. Proc Natl Acad Sci U S A. **103**(29): 11051-6.

Duennwald, M. L., Jagadish, S., Muchowski, P. J. and Linquist, S. 2006b. Flanking sequences profoundly alter polyglutamine toxicity in yeast. Proc Natl Acad Sci U S A. **103**(29): 11045-50.

Duyao, M., *et al.* 1993. Trinucleotide repeat length instability and age of onset in Huntington's disease. Nat Genet. **4**(4): 387-92.

Ferro, A., *et al.* 2007. NEDD8: a new ataxin-3 interactor. Biochim Biophys Acta. **1773**(11): 1619-27.

Galdieri, L., Mehrotra, S., Yu, S. an Vancura, A. 2010. Transcriptional regulation in yeast during diauxic shift and stationary phase. OMICS. **14**(6): 629-38.

Gao, X. and Hu, H. 2008. Quality control of the proteins associated with neurodegenerative diseases. Acta Biochim Biophys Sin (Shanghai). **40**(7): 612-8.

Gari, E., Piedrafita, L., Aldea, M. and Herrero, E. 1997. A set of vectors with a tetracycline-regulatable promoter system for modulated gene expression in Saccharomyces cerevisiae. Yeast. **13**(9): 837-48.

Goffeau, A., *et al*. 1996. Life with 6000 genes. Science. **274**(5287): 546, 563-7.

Goto, J., *et al.* 1997. Machado-Joseph disease gene products carrying different carboxyl termini. Neurosci Res. **28**(4): 373-7.

Guo, M. 2010. What have we learned from Drosophila models of Parkinson's disease? Prog Brain Res. **184**: 3-16; Chapter 1.

Gusella, J. F., *et al.* 1983. A polymorphic DNA marker genetically linked to Huntington's disease. Nature. **306**(5940): 234-8.

Haacke, A., Broadley, S. A., Boteva, R., Tzvetkov, N. Hartl, F. U. and Breuer, Peter. 2006. Proteolytic cleavage of polyglutamine-expanded ataxin-3 is critical for aggregation and sequestration of non-expanded ataxin-3. Hum Mol Gen. **15**(4): 555-568.

Høyer-Hansen, M. and Jäättelã, M. 2007. Connecting endoplasmic reticulum stress to autophagy by unfolded protein response and calcium. Cell Death Differ. **14**(9): 1576-82.

Hughes, R. E., Lo, R. S., Davies, C., Strand, A. D., Neal, C. L., Olson, J. M. and Fields, S. 2001. Altered transcription in yeast expressing expanded polyglutamine. PNAS. **98**(23): 13201-13206.

Ichikawa, Y., *et al.* 2001. The genomic structure and expression of MJD, the Machado-Joseph disease gene. J Hum Genet. **46**(7): 413-22.

Jana, N. R., Zemskov, E. A., Wang, G. and Nukina, N. 2001. Altered proteasomal function due to the expression of polyglutamine-expanded truncated N-terminal huntingtin induces apoptosis by caspase activation through mitochondrial cytochrome c release. Hum Mol Genet. **10**(10): 1049-59.

Kaeberlein, M., Burtner, C. R. and Kennedy, B. K. 2007. Recent developments in yeast aging. PLoS Genet. **3**(5): e84.

Kawai, Y., Takeda, A., Abe. Y., Washimi, Y., Tanaka, F. and Sobue, S. 2004. Cognitive impairments in Machado-Joseph disease. Arch Neurol. **61**(11): 1757-60.

Kawaguchi, Y., *et al.* 1994. CAG expansions in a novel gene for Machado-Joseph disease at chromosome 14q32.1. Nat Genet. **8**(3): 221-8.

Khan, L. A., Yamanaka, T. and Nukina, N. 2008. Genetic impairment of autophagy intensifies expanded polyglutamine toxicity in Caenorhabditis elegans. Biochem Biophys Res Commun. **368**(3): 729-35.

Kraft, C., Reggiori, F. and Peter, M. 2009. Selective types of autophagy in yeast. Biochim Biophys Acta. **1793**(9): 1404-12.

Krobibitsch, S. and Linquist, S., 1999. Aggregation of huntingtin in yeast varies with the length of the polyglutamine expansion and the expression of chaperone proteins. PNAS. 97(4):1589-1594.

Kundu, M. and Thompson, C. B. 2008. Autophagy: basic principles and relevance to disease. Annu Rev Pathol. **3**: 427-55.

Landles, C. and Bates, G. P. 2004. Huntingtin and the molecular pathogenesis of Huntington's disease. Fourth in molecular medicine review series. EMBO Rep. **5**(10): 958-63.

Leavitt, B. R., Guttman, J. A., Hodgson, J. G., Kimel, G. H., Singaraja, R., Vogl, A. W. and Hayden, M. R. 2001. Wild-type huntingtin reduces the cellular toxicity of mutant huntingtin in vivo. Am J Hum Genet. **68**(2): 313-24.

Lee, C and Yu, M. 2005. Protein folding and diseases. Journal of Biochemistry and Molecular Biology. vol.38, pp 275-280.

Lehman, N. L. 2009. The ubiquitin proteasome system in neuropathology. Acta Neuropathol. **118**(3): 329-47.

Li, F., Macfarlan, T., Pittman, R. N. and Chakravartis, D. 2002. Ataxin-3 is a histone-binding protein with two independent transcriptional corepressor activities. J Biol Chem. **277**(47): 45004-12.

Link, C. D. 2001. Transgenic invertebrate models of age-associated neurodegenerative diseases. Mech Ageing Dev. **122**(14): 1639-49.

V. References

Maciel, P., *et al*. 1995. Correlation between CAG repeat length and clinical features in Machado-Joseph disease. Am J Hum Genet. **57**(1): 54-61.

Maiuri, M. C., Zalckvar, E., Kimchi 2, A. and Kroemer, G. 2007. Self-eating and self-killing: crosstalk between autophagy and apoptosis. Nat Rev Mol Cell Biol. **8**(9): 741-52.

Menzies, F. M., Huebener, J., Renna, M., Bonin, M., Reiss, O. and Rubinsztein, D. C. 2010. Autophagy induction reduces mutant ataxin-3 levels and toxicity in a mouse model of spinocerebellar ataxia type 3. Brain. **133**(Pt 1): 93-104.

Mizushima, N., Levine, B., Cuervo, A. M. and Klionsky, D. J. 2008. Autophagy fights disease through cellular self-digestion. Nature. **451**(7182): 1069-75.

Møllersen, L., Rowe, A. D., Larsen, E., Rognes, T and Klungland, A. 2010. Continuous and periodic expansion of CAG repeats in Huntington's disease R6/1 mice. PLoS Genet. **6**(12): e1001242.

Outeiro, T. F. and Lindquist, S. 2003. Yeast cells provide insight into alpha-synuclein biology and pathobiology. Science. **302**(5651): 1772-5.

Pan, T., Kondo, S., Zhu, W., Xie, W., Jankovic, J. and Le, W. 2008. Neuroprotection of rapamycin in lactacystin-induced neurodegeneration via autophagy enhancement. Neurobiol Dis. **32**(1): 16-25.

Paulson, H. L. 1997. Intranuclear Inclusions of Expanded Polyglutamine Protein in Spinocerebellar Ataxia Type 3. Neuron. **19**: 333–344

Paulson, H. L. 2007. Dominantly inherited ataxias: lessons learned from Machado-Joseph disease/spinocerebellar ataxia type 3. Semin Neurol. **27**(2): 133-42.

Rajawat, Y. S. and Bossis, I. 2008. Autophagy in aging and in neurodegenerative disorders. Hormones (Athens). **7**(1): 46-61.

Rockabrand, *et al*. 2006. The first 17 amino acids of Huntingtin modulate its sub-cellular localization, aggregation and effects on calcium homeostasis. Human Molecular Genetics. **16**(1):61-77.

Ross, C. A., *et al*., 1999. Polyglutamine pathogenesis. Philos Trans R Soc Lond B. **354**(1386): 1005-11.

Rubinsztein, D. C. 2008. Functional genomics approaches to neurodegenerative diseases. Mamm_Genome. **19**(9): 587-90.

Sambrook J, Fritsch EF, Maniatis T., 1989. Molecular cloning: a laboratory manual. Cold Spring Harbor Laboratory, Cold Spring Harbor, New York.

Sang, T. and Jackson, G. R. 2005. Drosophila Models of Neurodegenerative Diseases. The J Ame Soci Exp NeuroThe. **2**: 438-446.

Silva-Fernandes, A. *et al*., 2010 Motor uncoordination and neuropathology in a transgenic mouse model of Machado-Joseph disease lacking intranuclear inclusions and ataxin-3 cleavage products. Neurobiol Dis. **40**(1): 163-76.

Solans, A., Zambrano, A., Rodriíguez, M. and Barrientos, A. 2006. Cytotoxicity of a mutant huntingtin fragment in yeast involves early alterations in mitochondrial OXPHOS complexes II and III. Hum Mol Genet. **15**(20): 3063-81.

Takiyama, Y. *et al*. 1993. The gene for Machado-Joseph disease maps to human chromosome 14q. Nat Genet. **4**(3): 300-4.

Tenreiro, S. and Outeiro, T. F. 2010. Simple is good: yeast models of neurodegeneration. FEMS Yeast Res. **10**(8): 970-9.

The Huntington's Disease Collaborative Research Group, 1993. A novel gene containing a trinucleotide repeat that is expanded and unstable on Huntington's disease chromosomes. Cell. **72**(6): 971-83.

Truant, R. 2003. Nucleocytoplasmic transport of huntingtin and Huntington's disease. Clinicaln Neurosci Res. **3**: 157-164.

Truant, R., Atwal, R. S. and Burtnik, A. 2006. Nucleocytoplasmic trafficking and transcription effects of huntingtin in Huntington's disease. Prog Neurobiol. **83**(4): 211-27.

Tsai, H., Tsai H. and Hsieh, M. 2004. Full-length expanded ataxin-3 enhances mitochondrial-mediated cell death and decreases Bcl-2 expression in human neuroblastoma cells. Biochem Biophys Res Commun. **324**(4): 1274-82.

van Ham, T. J., Breitling, R., Swetz, M. A. and Nollen, E. A. A. 2009. Neurodegenerative diseases: Lessons from genome-wide screens in small model organisms. EMBO Mol Med. **1**(8-9): 360-70.

Vellai, T., 2009. Autophagy genes and ageing. Cell Death Differ. **16**(1): 94-102.

Winderickx, J., Delay, C., De Vos, Ann., Klinger, H., Pellens, K., Vanhelmont, T., Van Leuven, F. and Zabrocki, P. 2008. Protein folding diseases and neurodegeneration: Lessons learned from yeasts. Biochi Bioph Acta. **1738**: 1381-1395.

Zhai, W., Jeong, H., Cui, L., Krainc, D. and Tjian, R. 2005. In vitro analysis of huntingtin-mediated transcriptional repression reveals multiple transcription factor targets. Cell. **123**(7): 1241-53.

Zhong, X. and Pittman, R. N. 2006. Ataxin-3 binds VCP/p97 and regulates retrotranslocation of ERAD substrates. Hum Mol Genet. **15**(16): 2409-20.